Electronic Supplementary Material (ESI) for Nanoscale.

Supporting Information

Light harvesting porphyrazines to enable intramolecular singlet fission

Diana-Paola Medina,‡[a] Ilias Papadopoulos,‡[b] Giulia Lavarda,[a] Henrik Gotfredsen,[c] Parisa R. Rami,[d] Rik R. Tykwinski,*[d] M. Salomé Rodríguez-Morgade,*[a,e] Dirk M. Guldi*[b] and Tomás Torres*[a,e,f]

[a] *Departamento de Química Orgánica, Universidad Autónoma de Madrid, Cantoblanco, 28049 Madrid (Spain). E-mail: salome.rodriguez@uam.es (M.S.R.-M.); tomas.torres@uam.es (T.T.)*

[b] *Department of Chemistry and Pharmacy & Interdisciplinary Center for Molecular Materials (ICMM), University of Erlangen-Nuremberg, Egerlandstraße 3, 91058 Erlangen, (Germany). E-mail: dirk.guldi@fau.de (D.M.G.)*

[c] *Department of Chemistry, University of Copenhagen, Universitetsparken 5, DK-2100 Copenhagen, Denmark.*

[d] *Department of Chemistry, University of Alberta, Edmonton, Alberta, T6G 2G2, Canada. E-mail: rik.tykwinski@ualberta.ca (R.R.T.)*

[e] *Institute for Advanced Research in Chemical Sciences (IAdChem), Universidad Autónoma de Madrid , Cantoblanco, 28049 Madrid, Spain.*

[f] *IMDEA-Nanociencia. c/ Faraday 9, Cantoblanco, 28049 Madrid (Spain).*

Electronic Supplementary Information (ESI) available: [details of any supplementary information available should be included here]. See DOI: 10.1039/x0xx00000x

‡ These authors contributed equally to this work.

General Procedures, Materials, and Methods

Synthesis and characterization

Steady-state UV-Vis absorption spectra (λ_{max} and ε) were acquired with a V-660 UV-Vis spectrophotometer (Jasco) at room temperature (rt). MALDI-TOF MS spectra were obtained from a BRUKER ULTRAFLEX III instrument equipped with a nitrogen laser operating at 337 nm and recorded in the positive-polarity mode. A convenient matrix for these measurements is indicated for each compound. NMR spectra were recorded with a BRUKER Avance-300 (300 MHz) and a BRUKER DRX-500 (500 MHz) spectrometer. The temperature was actively controlled at 298 K. In the ^{1}H-NMR and ^{13}C-NMR spectra, the chemical shifts (δ) are measured in ppm relative to tetramethylsilane. Column chromatography was carried out on silica gel Merck-60 (230-400 mesh, 60 Å) and TLC was performed on aluminum sheets precoated with silica gel 60 F254 (Merck). Size exclusion chromatography was performed on Bio-BeadsTM S-X1 Support (200-400 mesh). **PzCOOH,**[1] **Pnc$_2$COOH**[2] and **Pnc$_2$OH**[3] were synthesized as previously reported. The other chemicals were purchased from commercial suppliers and used without further purification. Dry solvents were purchased from commercial suppliers in anhydrous grade or thoroughly dried before use employing standard methods.

Photophysical Studies

Steady-State Absorption and Emission. Steady-state UV-vis absorption measurements were carried out at on a Perkin Elmer Lambda 2 spectrometer or a Varian Cary 5000 UV-vis-NIR spectrophotometer at room temperature (rt). Steady-state emission spectra were recorded with a FluoroMax3 spectrometer from Horiba in the visible detection range (rt). The data was recorded using FluorEssence software from Horiba Jobin Yvon. Fluorescence quantum yields (Φ_F) were determined by means of gradient analyses using cresyl violet perchlorate ($\Phi_F = 0.54$) in ethanol for the ZnPz fluorescence and zinc phthalocyanine ($\Phi_F = 0.30$) in toluene for the Pnc$_2$ fluorescence. All measurements were performed in 10 x 10 mm quartz cuvettes at rt.

Time-Correlated Single Photon Counting (TCSPC). Fluorescence lifetimes were determined by the time-correlated single photon counting (TCSPC) technique using a FluoroLog3 emission spectrometer (Horiba JobinYvon) equipped with an R3809U-58 MCP (Hamamatsu) and an EXW-6 (NKT) SuperK Extreme highpower supercontinuum fiber laser with excitation at 570 and 633 nm (~150 ps fwhm).

Femtosecond and Nanosecond Transient Absorption Spectroscopy. Femtosecond (0 to 5250 ps) and nanosecond (1 ns to 400 µs) transient absorption experiments (fsTA and nsTA) were carried out with an amplified Ti:sapphire CPA-2110 fs laser system (Clark MXR: output 775 nm, 1 kHz, 150 fs pulse width) using transient absorption pump/probe detection systems (Helios and Eos, Ultrafast Systems) with argon purged solutions (~15 minutes) in 2 x 10 mm cuvettes. The 570 and 633 nm excitation wavelengths, with energies of 400 nJ, respectively, were generated with a noncolinear optical parametric amplifier (NOPA, Clark MXR). Transient absorption spectra were recorded using transient absorption pump-probe detection systems (HELIOS and EOS, Ultrafast Systems). A homogenous excitation of the probed area was ensured, by keeping the spot diameter of the pump beam always larger than that of the probe beam. A controlled delay stage (fsTA) or electronic response (nsTA) was responsible for the delay of the probe pulses with respect to the pump pulses. A beam splitter was used to split the probe pulses into two (signal and reference beam) before passing the sample. The probe and reference beam were detected independently to correct for fluctuations in the probe beam intensity. A reasonable signal-to-noise ratio for the transient spectra were acquired shot-by-shot and averaged at each delay (~1500 times).

Data Analysis. Data evaluation of the fsTa and nsTA data has been conducted by means of multiwavelength and GloTarAn global analysis. Global analysis was performed on the TA data sets using the proposed sequential model. The analytical solution to the coupled differential equations that describe the kinetic model is convoluted with a Gaussian instrument response function. After the least-squares fitting has converged, the raw data matrix is deconvoluted using the specific solution to the kinetic model and parameters from the fit to obtain the evolution-associated spectra and their populations as a function of time. GloTarAn is a Java-based graphical user interface to the R-package TIMP, which was developed for global and target analysis of time-resolved spectroscopy data. The dispersion (chirp of the white-light pulse) of the instrument response function (IRF) was modeled (Surface Xplorer by Ultrafast Systems) and taken into account during the fitting procedure.

Triplet Quantum Yield (TQY) Determination. The TQY determination was performed by following the same procedure from previous works. In short, for the TQY determination the intensification of the Pnc_2 related ground state bleach (GSB) was utilized. Further corrections of the EAS of the Pnc_2 were necessary, in order to account for residual contributions from the ZnPzs (e.g. GSB, fluorescence). The ratios between the singlet excited-state markers (~450 nm) and the minima of the GSBs of the Pnc_2 $^1(S_1S_0)$ states were matched to the resemble the respective Pnc_2 reference system (Pnc_2OH and Pnc_2COOH) in the respective solvent. For the calculation, the following **Equation (1)** was used:

$$\frac{\Delta OD_{EAS}(^1(T_1T_1)_{Pnc_2}}{\Delta OD_{EAS}(^1(S_1S_0)_{Pnc_2}} x\ 100\% = TQY$$

(1)

FRET Rate Constant Determination. For the calculation of the FRET rate constant the same procedure from previous works was applied, using the following **Equation (2)-(6)**:

$$R = R_0 \left(\frac{1-E}{E}\right)^{\frac{1}{6}} \tag{2}$$

R = FRET distance; R_0 = critical energy donor-acceptor distance; E = FRET efficiency.

$$E = 1 - \frac{\tau_{DA}}{\tau_D} \tag{3}$$

E = FRET efficiency; τ_{DA} = experimental lifetime (TA) of energy donor-acceptor conjugate; τ_D = experimental fluorescence lifetime of energy donor (TCSPC).

$$R_0 = 0.2108\left(\kappa^2 \Phi_F n^{-4} J\right)^{\frac{1}{6}} \tag{4}$$

R_0 = critical energy donor-acceptor distance; κ^2 = orientation factor; n = refractive index of the solvent; J = degree of spectral overlap.

$$J = \int_0^\infty F_D(\lambda)\varepsilon_A(\lambda)\lambda^4 d\lambda \tag{5}$$

J = degree of spectral overlap; F_D = fluorescence intensity of the donor at wavelength λ. The fluorescence spectra must be normalized to fulfill **Equation (6)**; ε_A = extinction coefficient of the acceptor at wavelength λ

$$\int_0^\infty F_D(\lambda) d\lambda = 1 \tag{6}$$

The detailed procedure (including a description of a software-based algorithm to calculate the spectral overlap integral J is described by HINK et al. For κ^2 we used 2/3 (~0.67), as often used for non-rigid systems ("dynamic isotropic limit"). The refractive indices n were taken as 1.496 and 1.528 for toluene and benzonitrile, respectively. See Table S1 for a summary of the parameters used for the FRET rate constant calculation as well as for an overview of the obtained values for the FRET constants.

Synthesis and Characterization

Scheme S1. Synthesis of **PzOH** and **PzCOOH**1

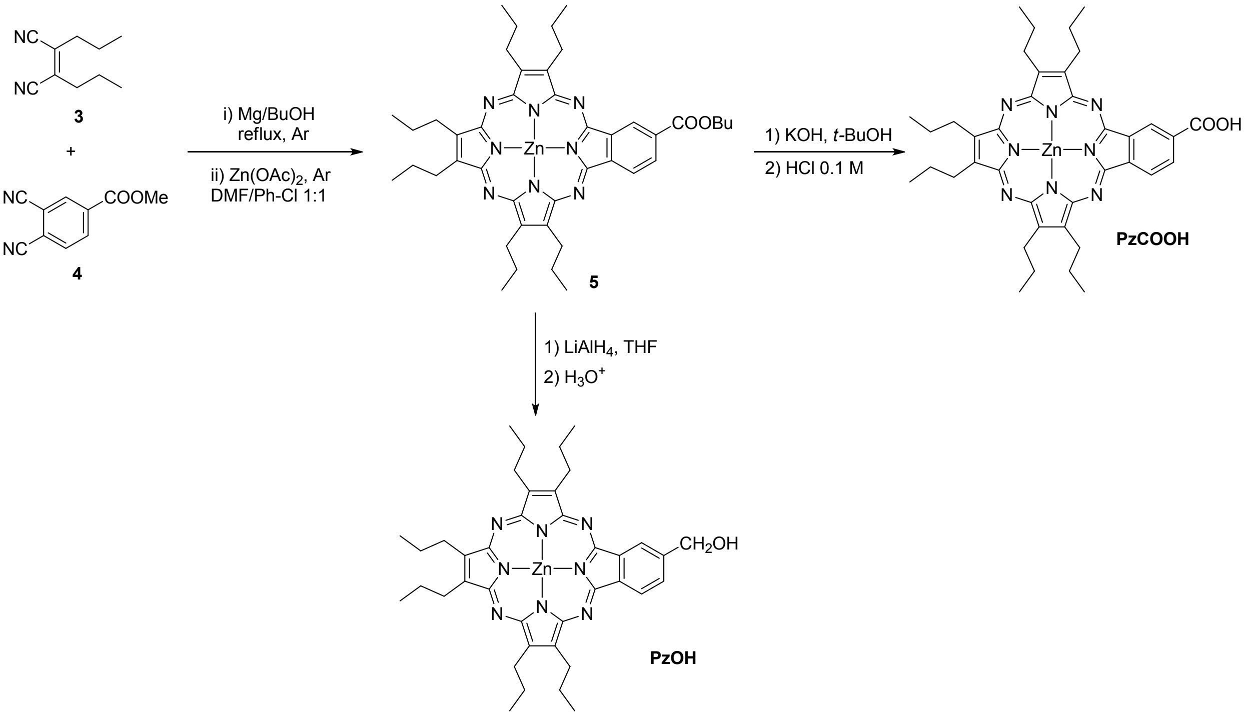

[2,3,7,8,12,13-(Hexapropyl)-17,18-(4'-butyloxycarbonylbenzo)-porphyrazinato] Zn(II) (5)

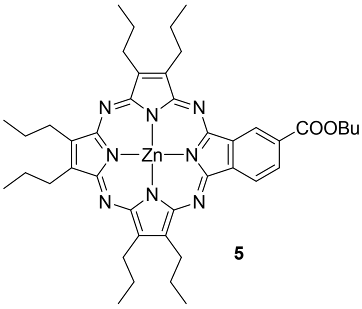

5

Magnesium turnings (51 mg, 2.1 mmol) and a spatula tip of iodine were heated in dry butanol (20 mL) under Ar for 8h. Then, dipropylmaleonitrile (**3**)[4] (340 mg, 2.1 mmol) and methyl 3,4-dicyanobenzoate (**4**)[5] (130 mg, 0.7 mmol) were added and the mixture was refluxed for 24h under argon. The solvent was rotary evaporated, and the residue was dissolved in TFA (20 mL) and left to stand at rt, protected from light, for 1h. The solution was poured over a 1:1 mixture of ice/NH_3 (30% aq.). The resulting precipitate was filtered and washed with water, a 1:1 mixture of methanol/water and finally, with methanol. After being dried, the solid was suspended in a 1:1 mixture of DMF/PhCl (20 mL), $Zn(OAc)_2$ (318 mg, 1.7 mmol) was added, and the mixture was heated at 140ºC for 8h. The solvent was rotary evaporated and the crude subjected to column chromatography on silica gel, using a 50:1 mixture of Toluene/THF as eluent, affording a blue solid (60 mg, 11%).

^{1}H-NMR (300 MHz, THF-d_8): δ(ppm) = 10.03 (s, 1H), 9.45 (d, *J* = 8.0 Hz, 1H), 8.81 (dd, *J* = 7.9, *J* = 1.4 Hz, 1H), 4.59 (t, *J* = 6.4 Hz, 2H), 4.1 – 3.8 (m, 12H), 2.43 (m, 12H), 2.1 – 1.9 (m, 4H), 1.4 - 1.2 (m, 18H), 1.15 (t, *J* = 7.4 Hz, 3H). UV-vis (THF): λ_{max} (nm) (log ε (dm^3 mol^{-1} cm^{-1})) = 633 (5.3), 578 (sh), 346 (5.0). MS (MALDI-TOF, DCTB): *m/z* = 778-785 [M]$^+$. HRMS: *m/z* = 778.3644. Calculated for ($C_{43}H_{54}N_8O_2Zn$): 778.3656.

[2,3,7,8,12,13-(Hexapropyl)-17,18-(4'-hydroxymethyl)-porphyrazinato] Zn(II) (PzOH)

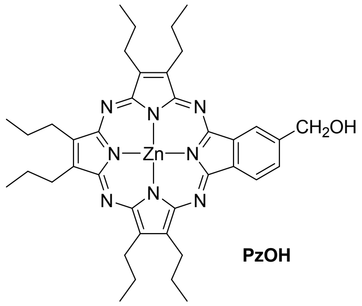

PzOH

To a stirred solution of **5** (50 mg, 0.06 mmol) in dry THF (1 mL) at rt, $LiAlH_4$ (0.08 mg, 0.08 mmol) was added in small portions. The reaction was monitored by TLC and when it was completed, NH_4Cl (1 mL) was added at 0 ºC. Next, HCl was added until pH = 2 and the solution was extracted with CH_2Cl_2 (5 x 5 mL). The organic layers were dried over Na_2SO_4. The solvent was rotary evaporated and the residue was chromatographed on silica gel using a 50:1 mixture of Toluene/THF as eluent. **PzOH** (20.5 mg, 45%), was obtained as a blue solid.

^{1}H-NMR (400 MHz, THF-d_8): δ(ppm) = 9.38 (s, 1H), 9.32 (d, *J* = 7.8 Hz, 1H), 8.15 (d, *J* = 7.8 Hz, 1H), 5.17 (d, *J* = 5.9 Hz, 2H), 4.72 (t, *J* = 5.9 Hz, 1H), 4.0 - 3.9 (m, 12H), 2.4 – 2.3 (m, 12H), 1.4 – 1.3 (m, 18H). ^{13}C-NMR (126 MHz, THF-d_8): δ(ppm) = 159.7, 159.6, 157.6, 157.5, 157.4, 156.2, 156.1, 146.2, 145.2, 144.0, 143.9, 143.8, 141.0, 139.6, 128.8, 123.2, 121.3, 65.5, 30.7, 29.2, 29.1, 29.0, 28.9, 26.7, 26.6, 26.5, 26.4, 15.2, 15.1. IR: ν(cm^{-1}) = 3337 (br, O-H), 2957, 2920, 2866 (C-H), 2656, 1462, 1371, 1151, 1013 (C-O), 952, 756, 728. UV-vis (THF): λ_{max} (nm) (log ε (dm^3 mol^{-1} cm^{-1})) = 618 (4.52), 604 (4.58), 572 (sh), 554 (3.86), 348 (4.78). MS (MALDI-TOF, DCTB): *m/z* = 708-714 [M]$^+$. HRMS: *m/z* = 708.3230; Calculated for ($C_{39}H_{48}N_8OZn$): 708.3237.

Scheme S2. Synthesis of **1** and **Pz1**

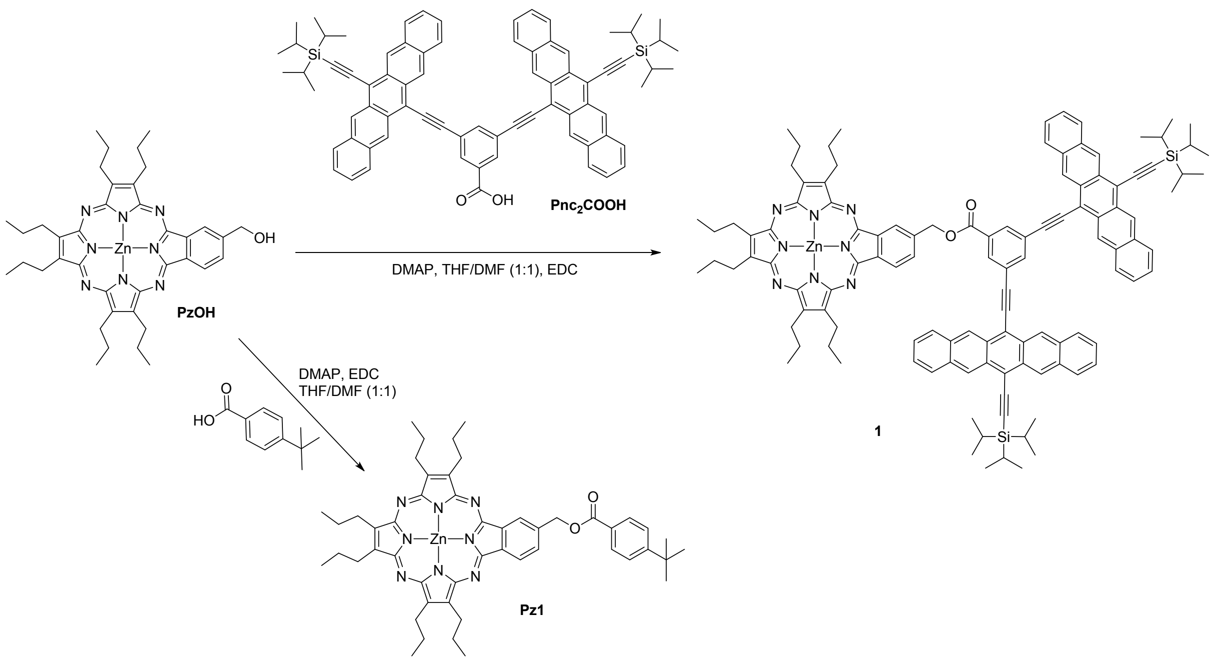

General Procedure for the preparation of 1, 2, Pz1 and Pz2

To a mixture of the carboxylic acid (0.04 mmol, 1 eq.), the alcohol (2.2 eq.) and DMAP (0.2 eq.) in a 1:1 mixture of THF/DMF (2 mL) at 0 ºC and under Ar, 1-ethyl-3-(3-dimethylaminopropyl)carbodiimide (EDC) (2.2 eq.) was added. The solution was stirred for 1 h and after, it was allowed to reach rt. After stirring at this temperature for 48 h, the mixture was washed with water and dried over $NaSO_4$. The solvent was rotary evaporated and the residue was chromatographed under the conditions specified for each compound.

Conjugate 1

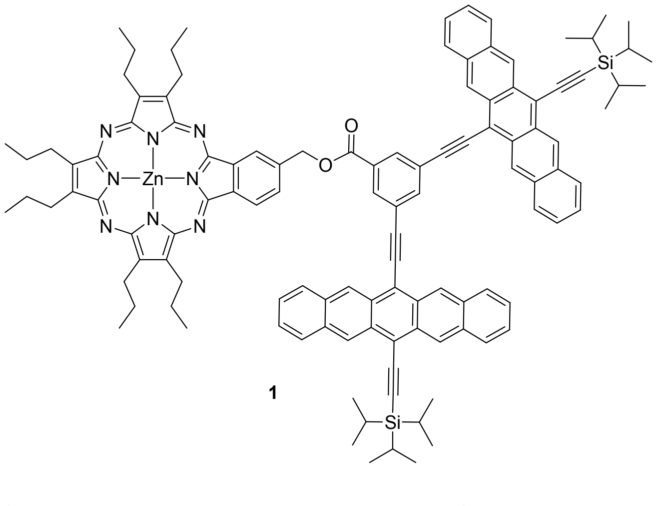

1

Starting from **PzOH** (41.29 mg, 0.034 mmol, 1.5 eq.). The compound was purified by gel permeation chromatography on Biobeads, using THF as the eluent, and then on silica gel using a 100:1 mixture of Toluene/THF. **1** was obtained as a blue solid (10.5 mg, 15%).

^{1}H-NMR (300 MHz, THF-d_8): δ (ppm) = 9.65 (s, 1H), 9.53 (d, J = 7.6 Hz, 1H), 9.39 (s, 4H), 9.25 (s, 4H), 8.86 (s, 2H), 8.81 (s, 1H), 8.51 (d, J = 7.7 Hz, 1H), 8.17 – 8.01 (m, 4H), 7.88 (m, 4H), 7.41 – 7.13 (m, 8H), 6.18 (s, 2H), 3.95 (m, 12H), 2.47 – 2.19 (m, 12H), 1.42 (s, 36H), 1.33 – 1.13 (m, 24H). ^{13}C-NMR (126 MHz, THF-d_8): δ (ppm) = 165.7, 157.8, 155.4, 145.2, 144.2, 144.0, 133.4, 131.4, 131.2, 130.7, 129.5, 129.2, 127.0, 126.8, 125.9, 123.8, 119.6, 118.2, 103.8, 90.3, 30.7, 29.2, 29.0, 28.9, 26.6, 26.5, 26.4, 25.9, 19.5, 15.2, 12.7. UV-vis (THF): λ_{max} (nm) (log ε ($dm^3\ mol^{-1}\ cm^{-1}$)) = 656 (3.6), 610 (4.1), 562 (3.4), 441 (sh), 435 (3.0), 347 (4.0), 308 (4.4). MS (MALDI-TOF, DCTB): m/z = 1772-1781 $[M]^+$. HRMS: m/z = 1772.8027; Calculated for ($C_{116}H_{116}N_8O_2Si_2Zn$): 1772.8046.

Pz1

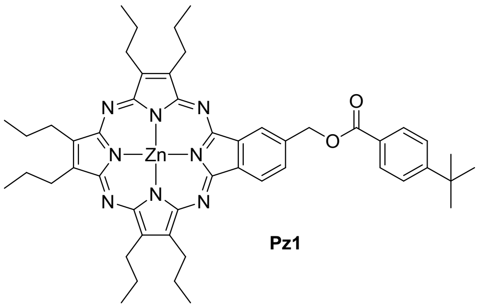

Pz1

Starting from **PzOH** (30 mg, 0.042 mmol, 1.5 eq.). The compound was chromatographed on silica gel using a 50:1 mixture of toluene/THF, affording **Pz1** as a blue solid (11 mg, 50%).

^{1}H-NMR (300 MHz, THF-d_8): δ (ppm) = 9.50 (s, 1H), 9.39 (d, J = 7.8 Hz, 1H), 8.29 (d, J = 7.7 Hz, 1H), 8.16 (d, J = 8.7 Hz, 2H), 7.61 – 7.54 (m, 2H), 5.95 (s, 2H), 4.05 – 3.86 (m, 12H), 2.46 – 2.29 (m, 12H), 1.36 (s, 9H), 1.33–1.25 (m, 18H). ^{13}C-NMR (76 MHz, THF-d_8): δ (ppm) = 166.6, 159.6, 159.5, 157.8, 157.7, 155.5, 155.4, 145.2, 144.2, 144.0, 140.9, 139.5, 130.4, 130.2, 128.9, 126.3, 123.6, 123.1, 122.7, 81.9, 36.0, 31.6, 29.0, 26.5, 15.2. UV-vis (THF): λ_{max} (nm) (log ε ($dm^3\ mol^{-1}\ cm^{-1}$)) = 616 (sh), 607 (4.91), 567 (sh), 556 (4.16), 348 (4.74). MS (MALDI-TOF, DCTB): m/z = 868 - 874 $[M]^+$. HRMS: m/z = 868.4102; Calculated for ($C_{50}H_{60}N_8O_2Zn$): 868.4125.

Scheme S3. Synthesis of **2** and **Pz2**

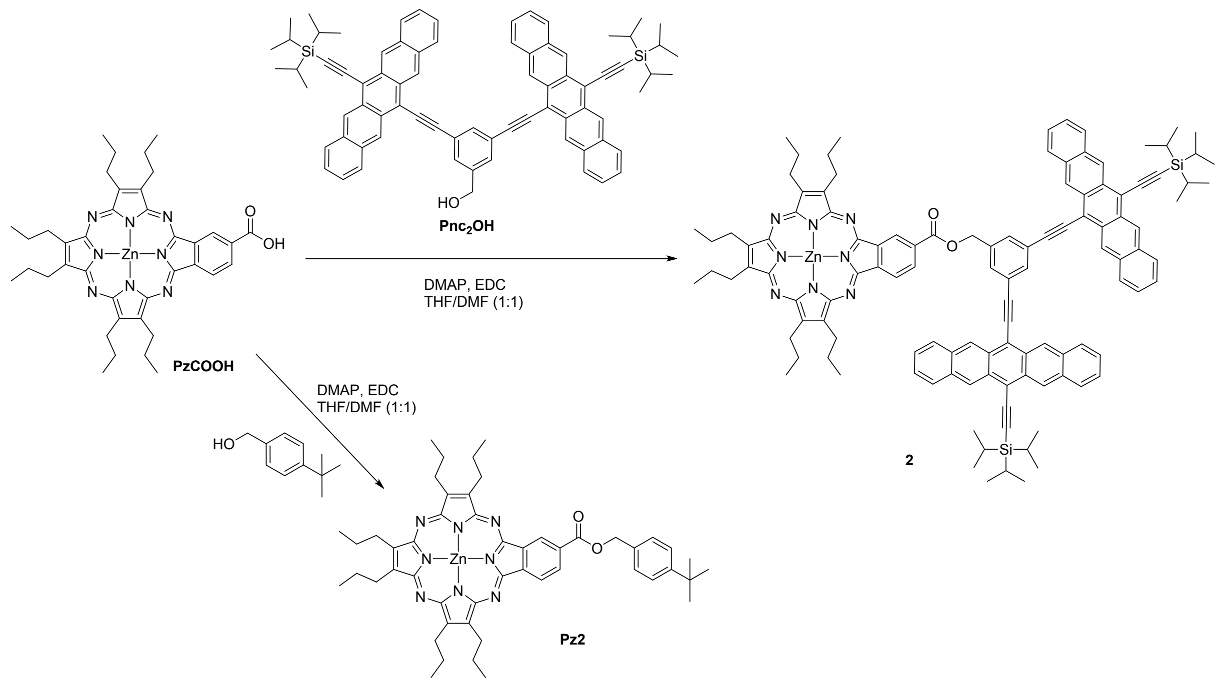

Conjugate 2

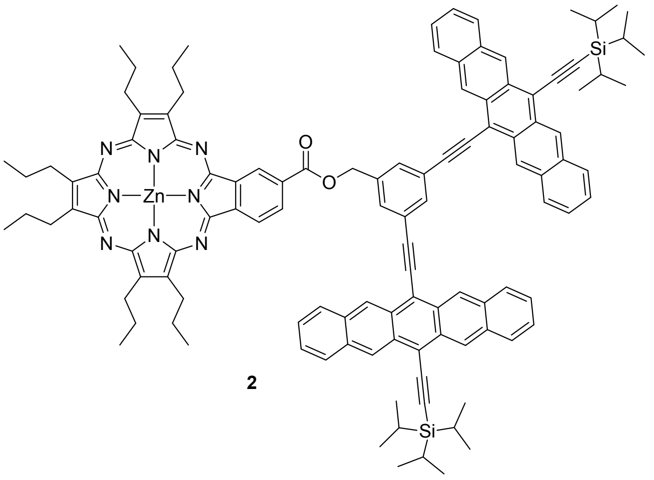

2

Starting from **PzCOOH** (30 mg, 0.041 mmol). The compound was chromatographed on Biobeads using THF as the eluent and then, on silica gel using a 100:1 mixture of Toluene/THF, affording **2** as a blue solid (15 mg, 20%).

^{1}H-NMR (300 MHz, THF-d_8): δ = 10.26 (s, 1H), 9.59 (d, J = 8.0 Hz, 1H), 9.53 (s, 4H), 9.35 (s, 4H), 9.08 (dd, J = 8.0, 1.5 Hz, 1H), 8.68 (t, J = 1.5 Hz, 1H), 8.48 (s, 2H), 8.21 – 8.12 (m, 4H), 7.98 – 7.90 (m, 4H), 7.32 (dd, J = 6.7, 3.1 Hz, 8H), 5.98 (s, 2H), 3.97-3.82 (m, 12H), 2.44 – 2.23 (m, 12H), 1.43 (s, 36H), 1.33 – 1.13 (m, 24H). ^{13}C-RMN (76 MHz, THF-d_8): δ (ppm) = 165.3, 150.2, 146.7, 140.5, 133.6, 133.5, 131.5, 131.3, 129.6, 129.2, 127.3, 127.0, 125.7, 104.8, 101.1, 29.3, 29.0, 26.6, 19.4, 15.2, 12.7. UV-vis (THF): λ_{max} (nm) (log ε (dm^3 mol^{-1} cm^{-1})) = 657 (4.37), 615 (4.80), 561 (4.12), 439 (9.63), 413 (3.75), 367 (4.55), 349 (4.63), 309 (5.22). MS (MALDI-TOF, DCTB): 1772-1781 [M]$^+$. HRMS: m/z = 1772.8038; Calculated for ($C_{116}H_{116}N_8O_2Si_2Zn$): 1772.8046.

Pz2

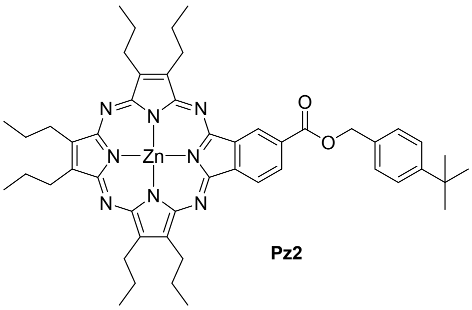

Pz2

Starting from **PzCOOH** (25 mg, 0.034 mmol). The compound was chromatographed on silica gel using a 50:1 mixture of heptane/AcOEt, affording a blue solid (15 mg, 50%).

^{1}H-NMR (300 MHz, THF-d_8): δ (ppm) = 10.05 (s, 1H), 9.44 (d, *J* = 7.9 Hz, 1H), 8.83 (dd, *J* = 8.0, 1.5 Hz, 1H), 7.69 – 7.49 (m, 4H), 5.60 (s, 2H), 4.05 – 3.92 (m, 12H), 2.46 – 2.32 (m, 12H), 1.38 (s, 9H), 1.35–1.25 (m, 18H). ^{13}C-NMR (76 MHz, THF-d_8): δ (ppm) = 167.0, 159.6, 159.4, 158.5, 158.3, 154.6, 154.1, 151.9, 145.4, 144.7, 144.6, 144.5, 144.3, 143.4, 140.2, 134.8, 132.1, 130.9, 129.2, 126.3, 125.1, 123.3, 35.3, 31.8, 29.1, 29.0, 28.9, 26.5, 15.2, 15.1. UV-vis (THF): λ_{max} (nm) (log ε (dm^3 mol^{-1} cm^{-1})) = 614 (4.9), 563 (4.2), 346 (4.6). MS (MALDI-TOF, DCTB): *m/z* = 868 - 875 [M]$^+$. HRMS: *m/z* = 868.4135; Calculated for ($C_{50}H_{60}N_8O_2Zn$): 868.4125.

Figure S1. ^{1}H NMR (THF-d_8) of **5**.

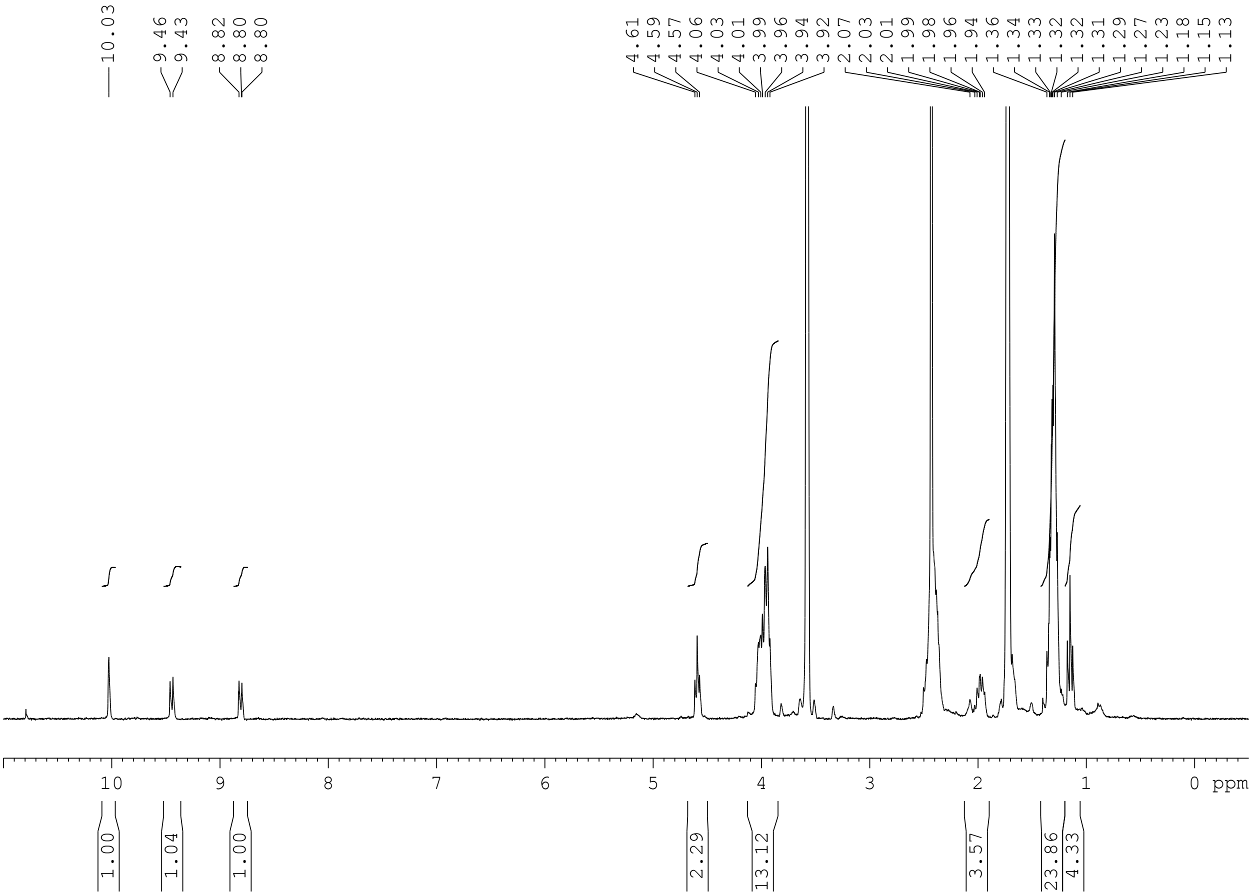

Figure S2. UV/Vis spectrum ($CHCl_3$) of **5**.

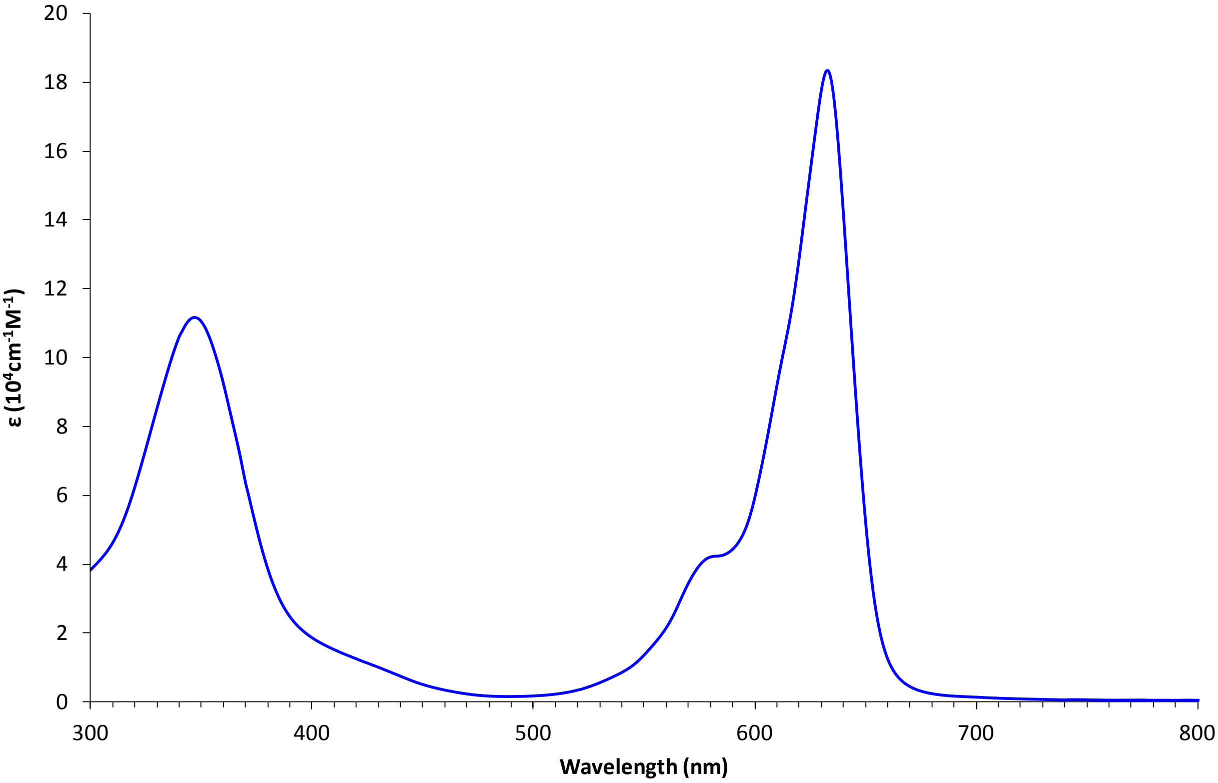

Figure S3. MS (MALDI-TOF) and HRMS spectra (inset) of **5**.

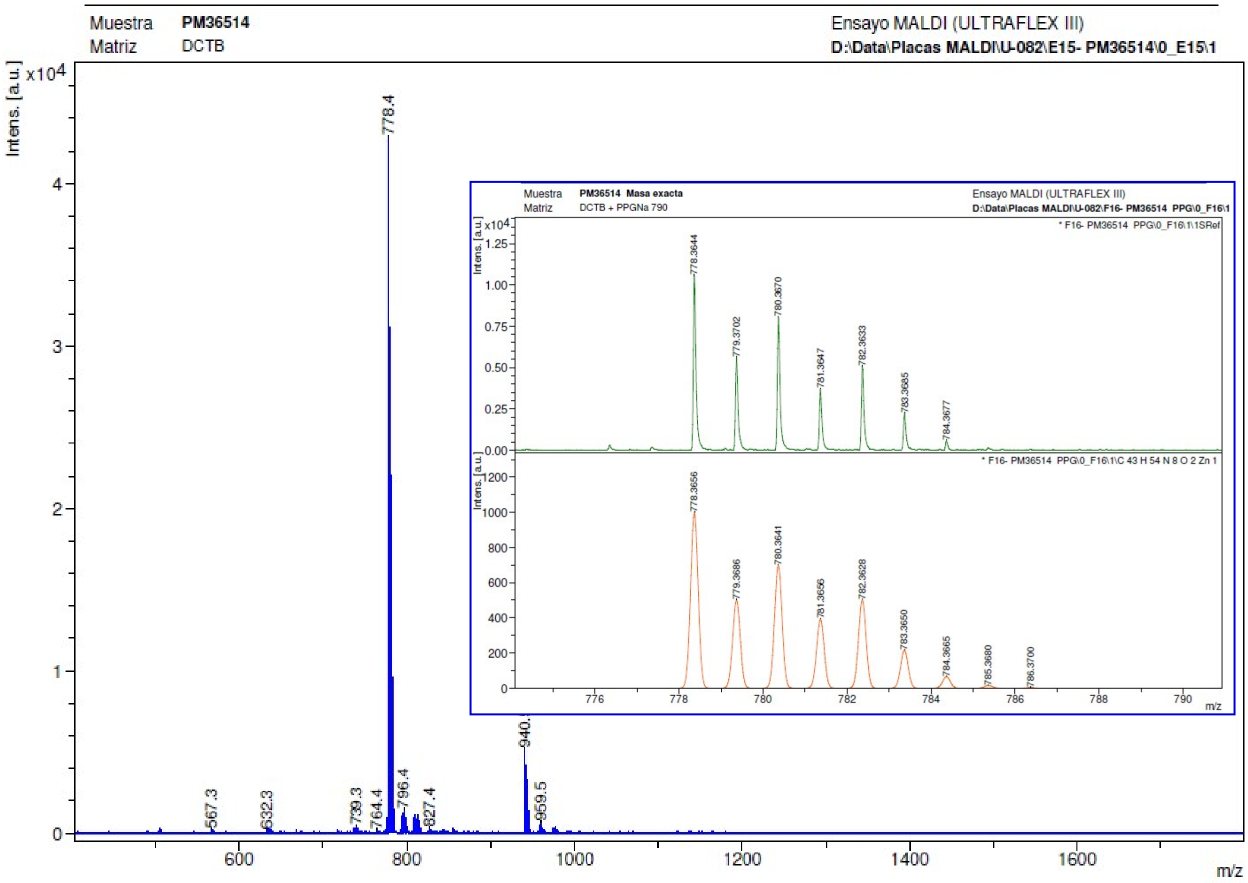

Figure S4. ^{1}H NMR (THF-d_8) of **PzOH**.

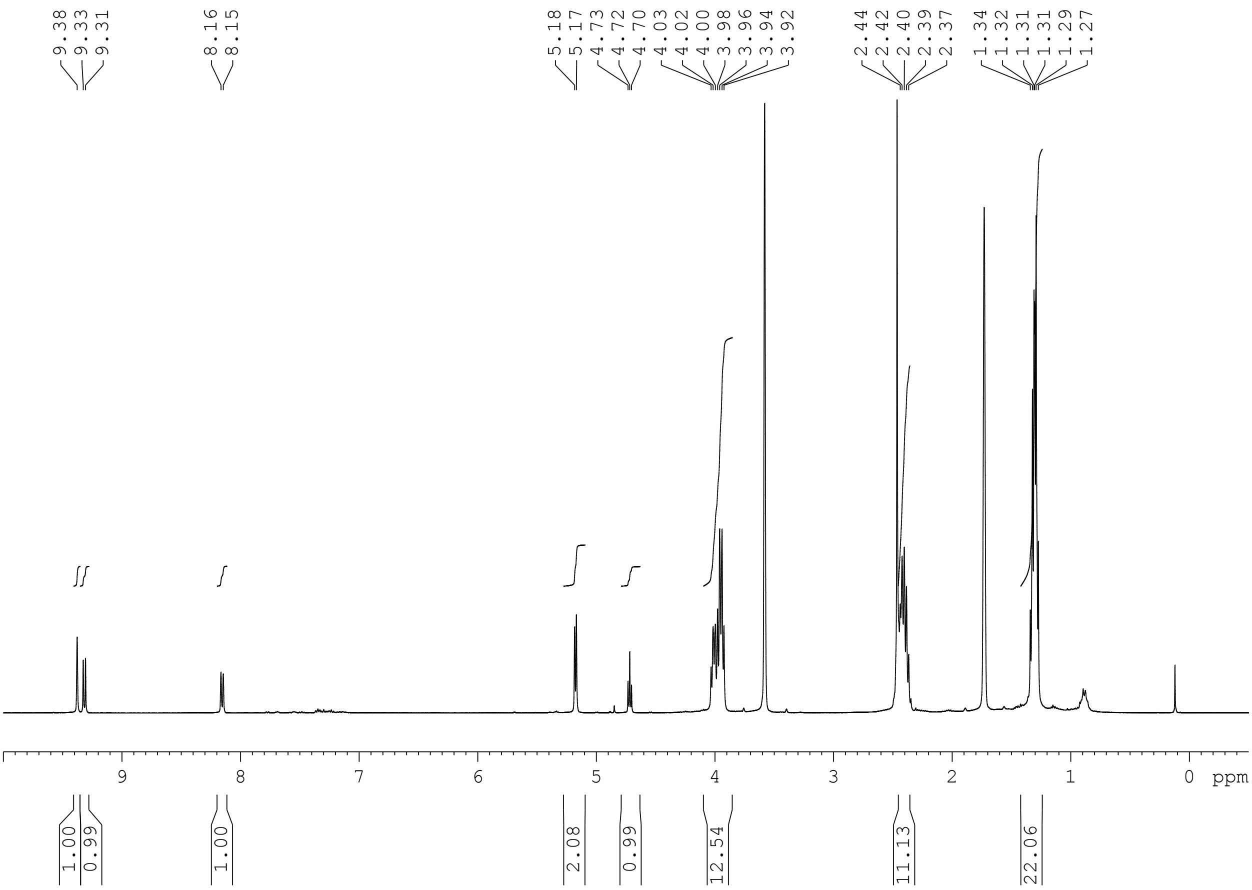

Figure S5. ^{13}C NMR (THF-d_8) of **PzOH**.

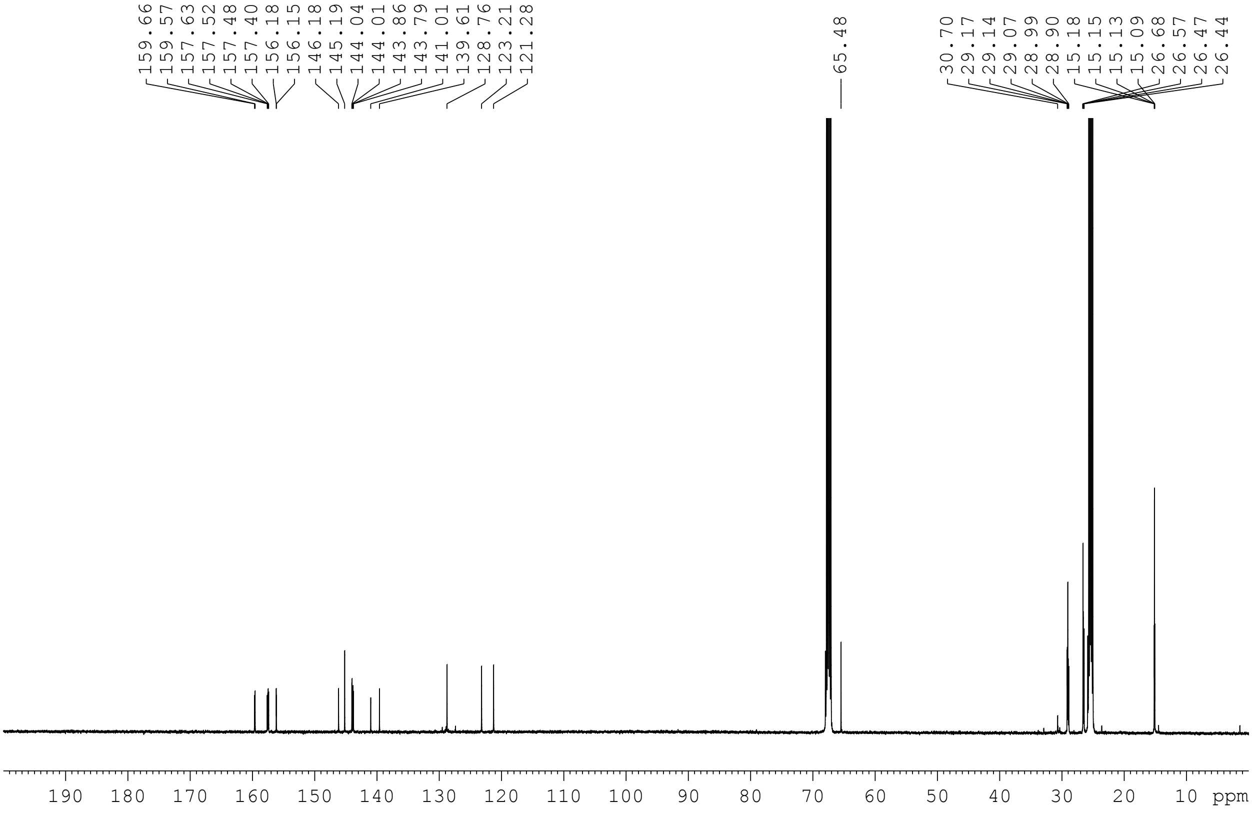

Figure S6. UV/Vis spectrum ($CHCl_3$) of **PzOH**.

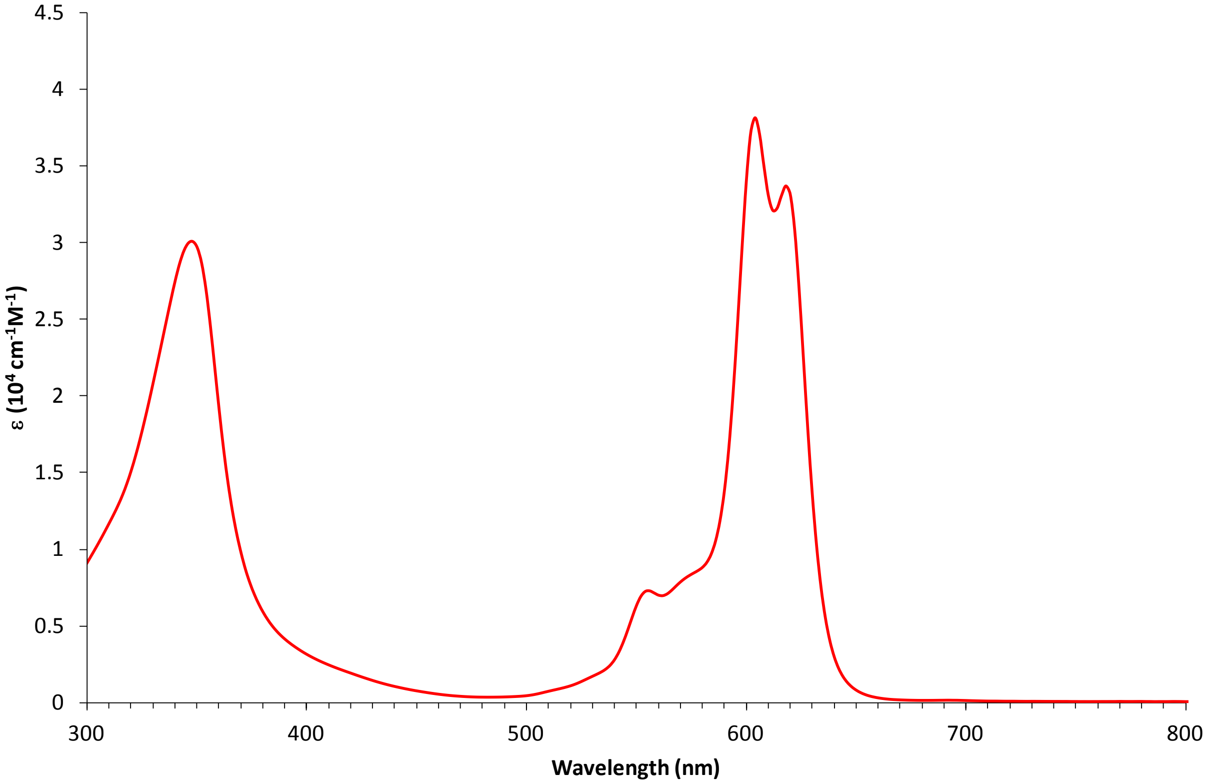

Figure S7. MS (MALDI-TOF) and HRMS spectra (inset) of **PzOH**.

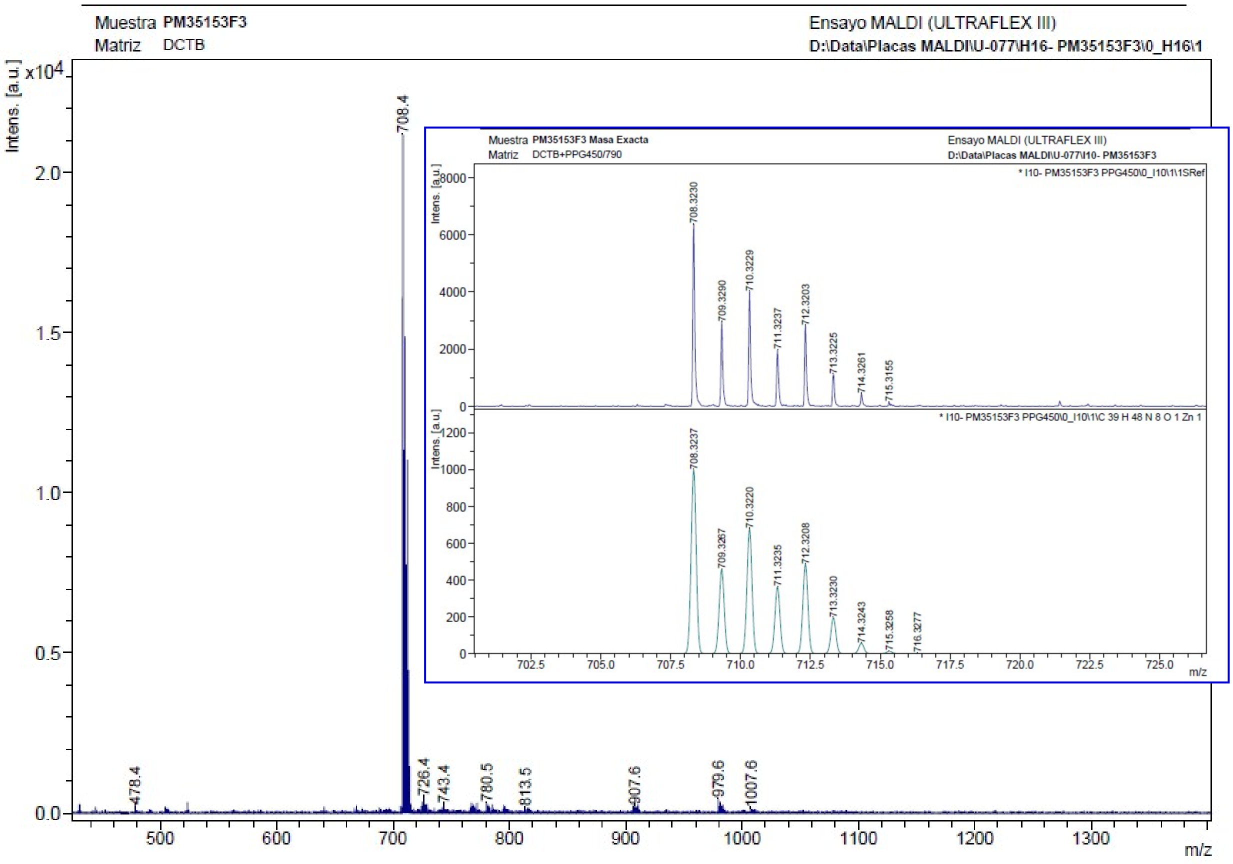

Figure S8. ^{1}H NMR spectra of a) **2** and b) **1** in d_8-THF.

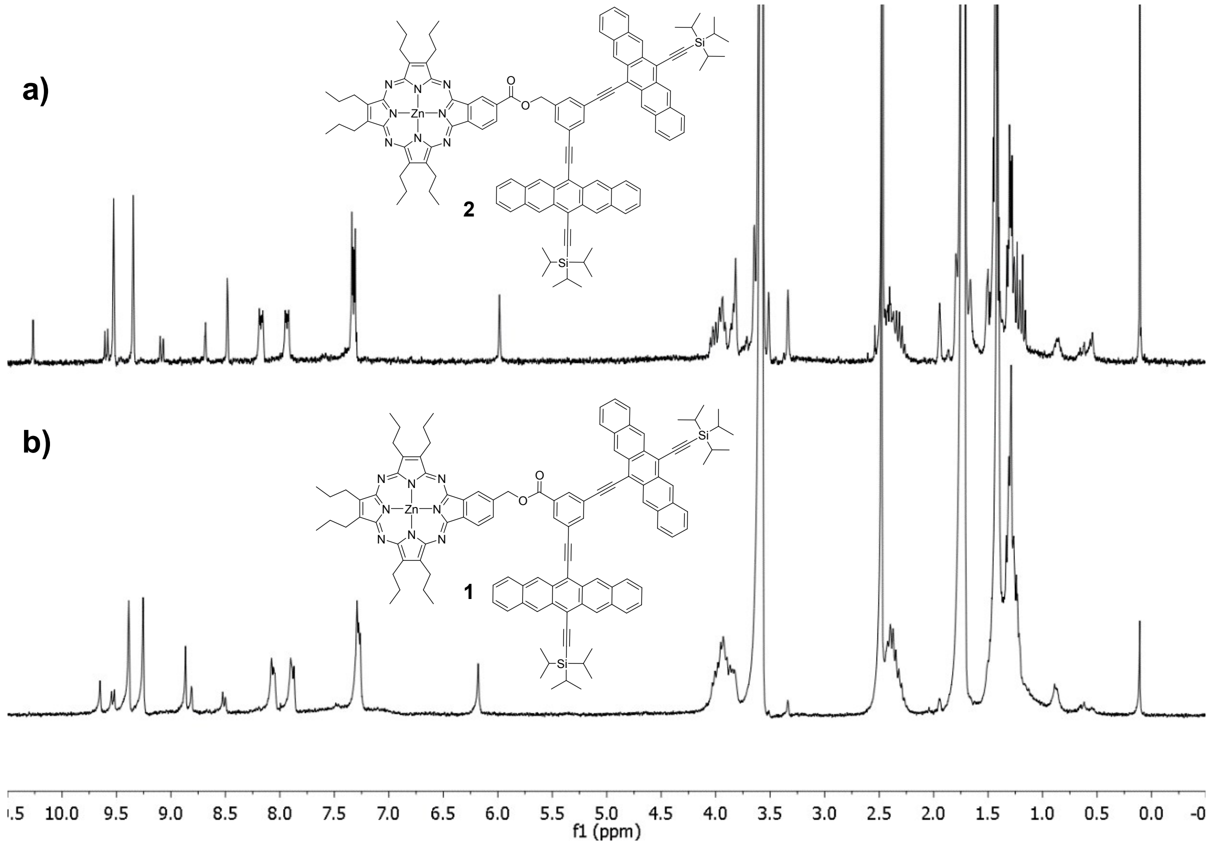

Figure S9. ^{13}C NMR spectra of **1** in d_8-THF.

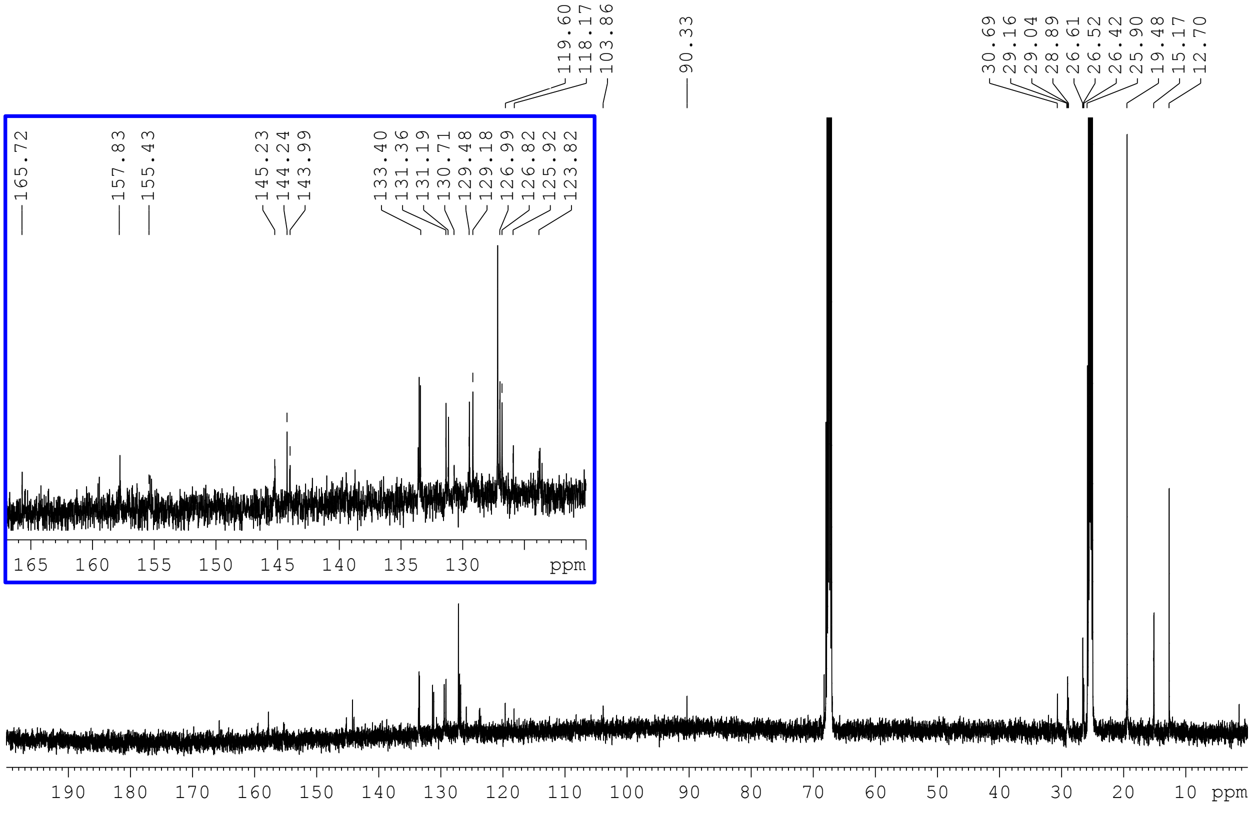

Figure S10. MS (MALDI-TOF) and HRMS spectra (inset) of **1**.

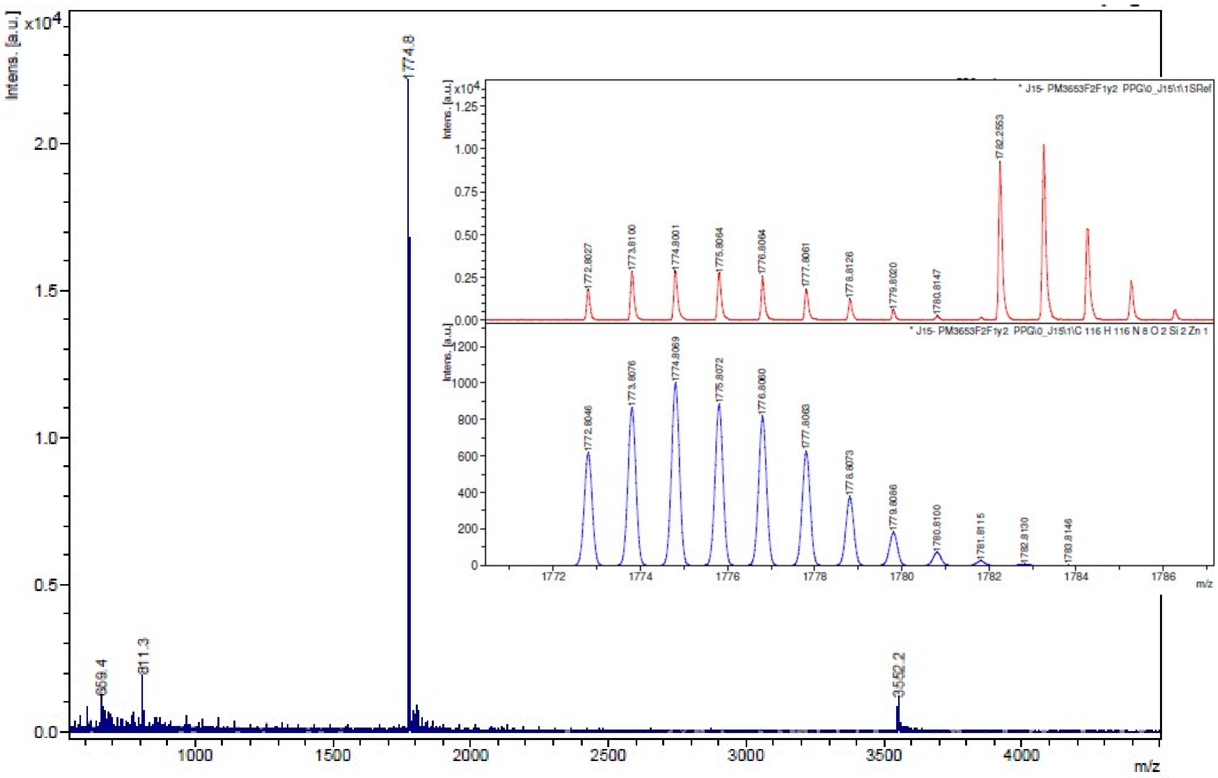

Figure S11. ^{13}C NMR spectra of **2** in d_8-THF.

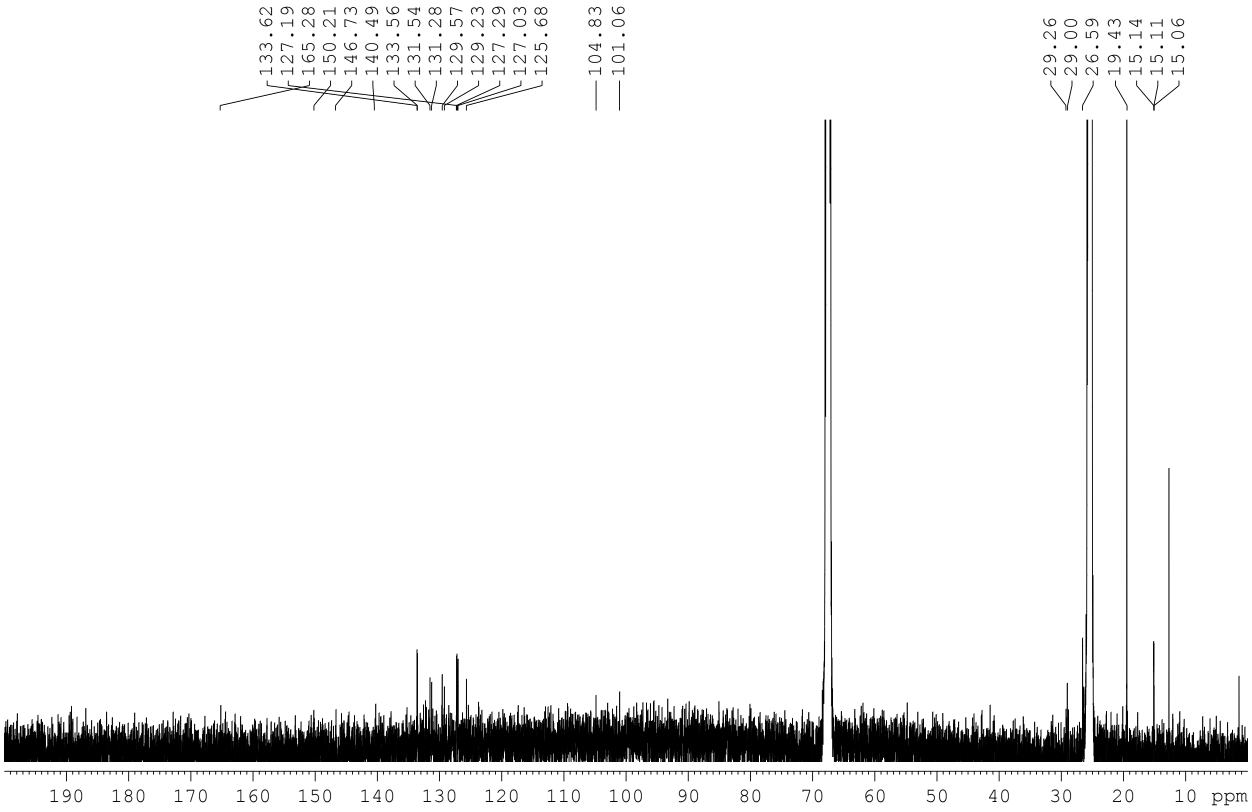

Figure S12. MS (MALDI-TOF) and HRMS spectra (inset) of **2**.

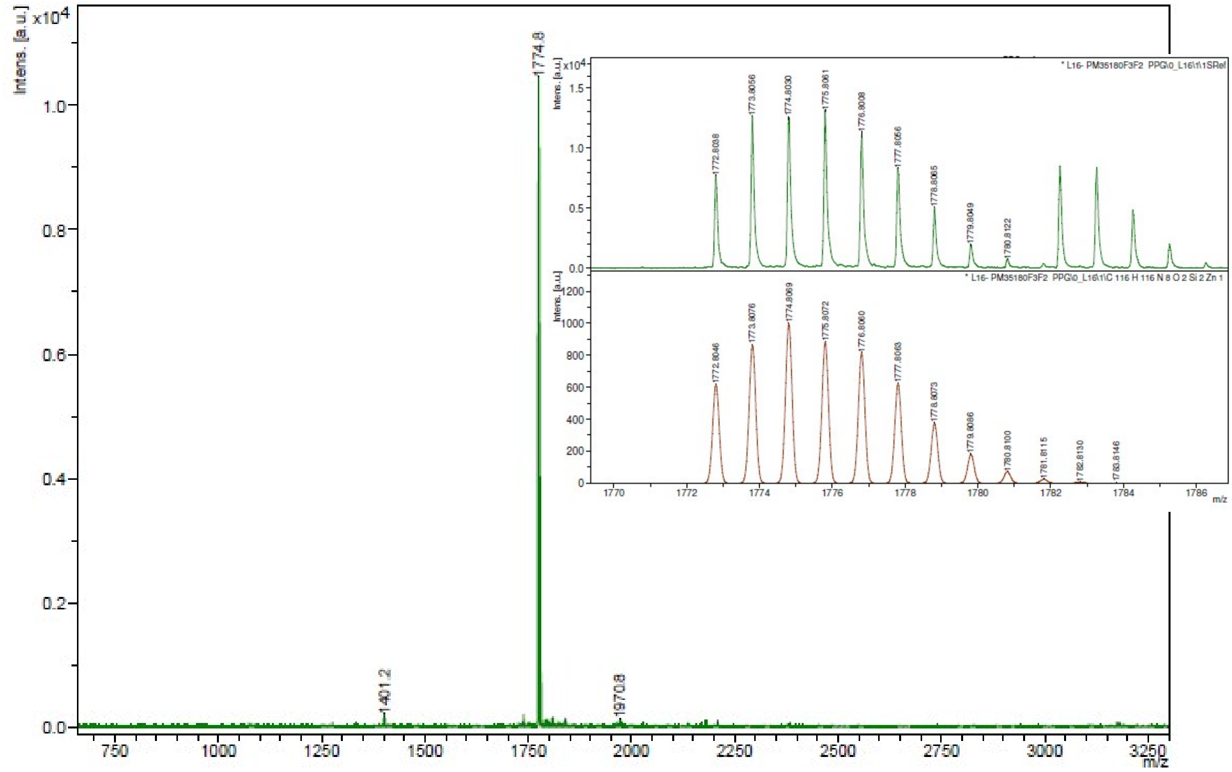

Figure S13. ^{1}H NMR spectra of a) **Pz2** and b) **Pz1** in d_8-THF.

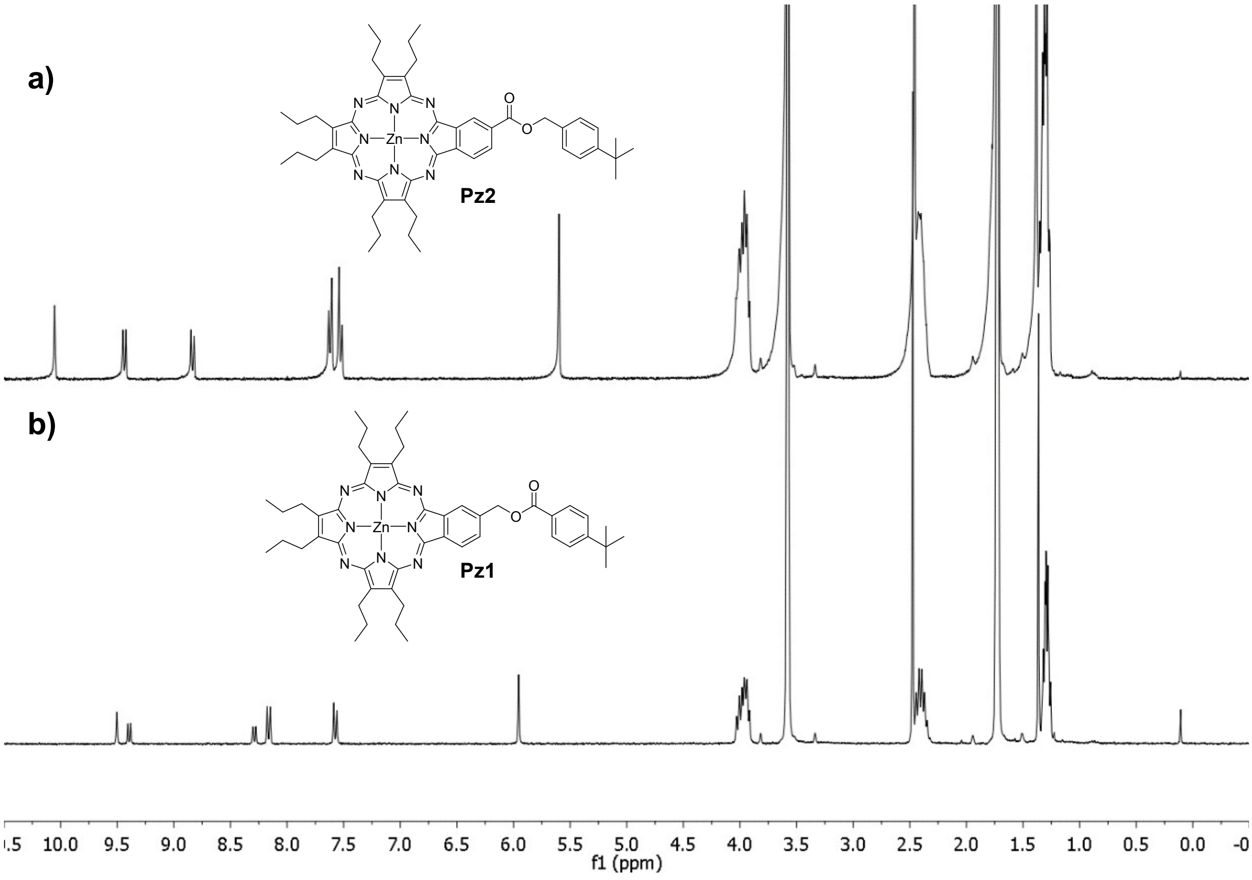

Figure S14. ^{13}C NMR spectra of **Pz1** in d_8-THF.

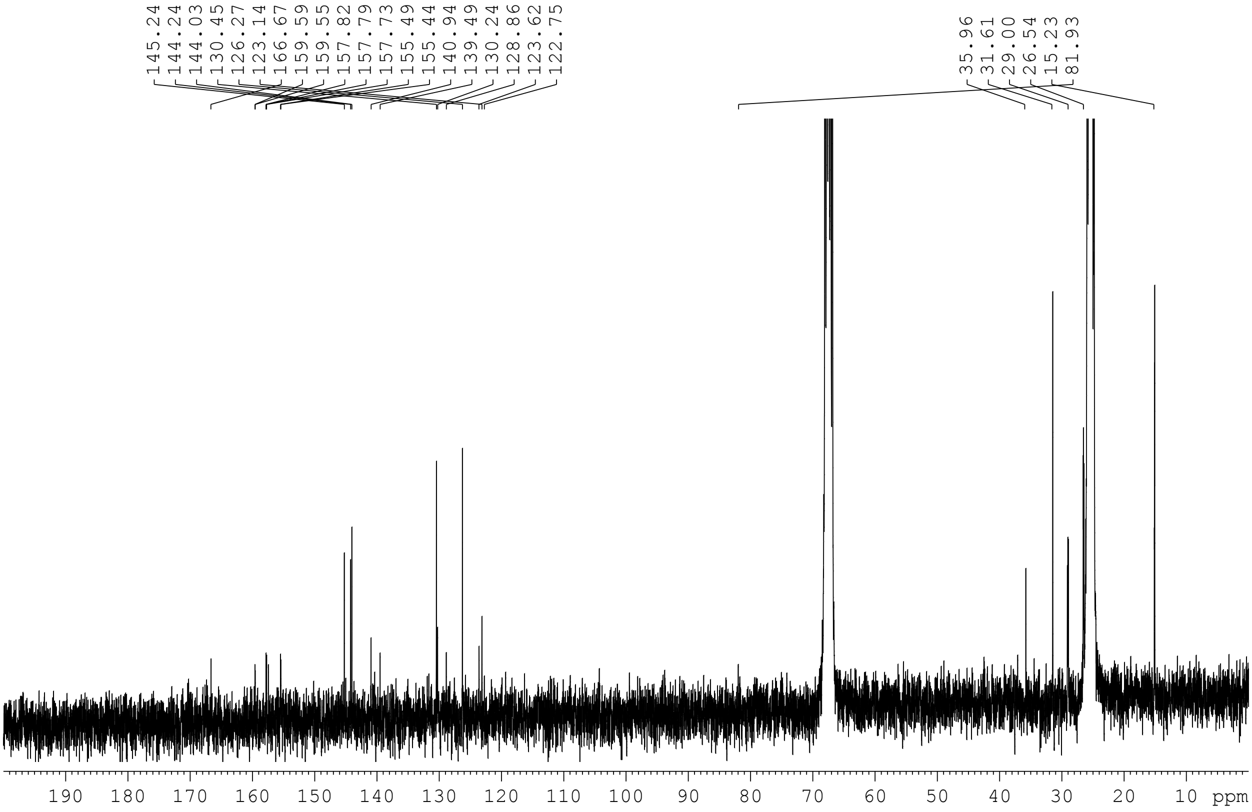

Figure S15. MS (MALDI-TOF) and HRMS spectra (inset) of **Pz1**.

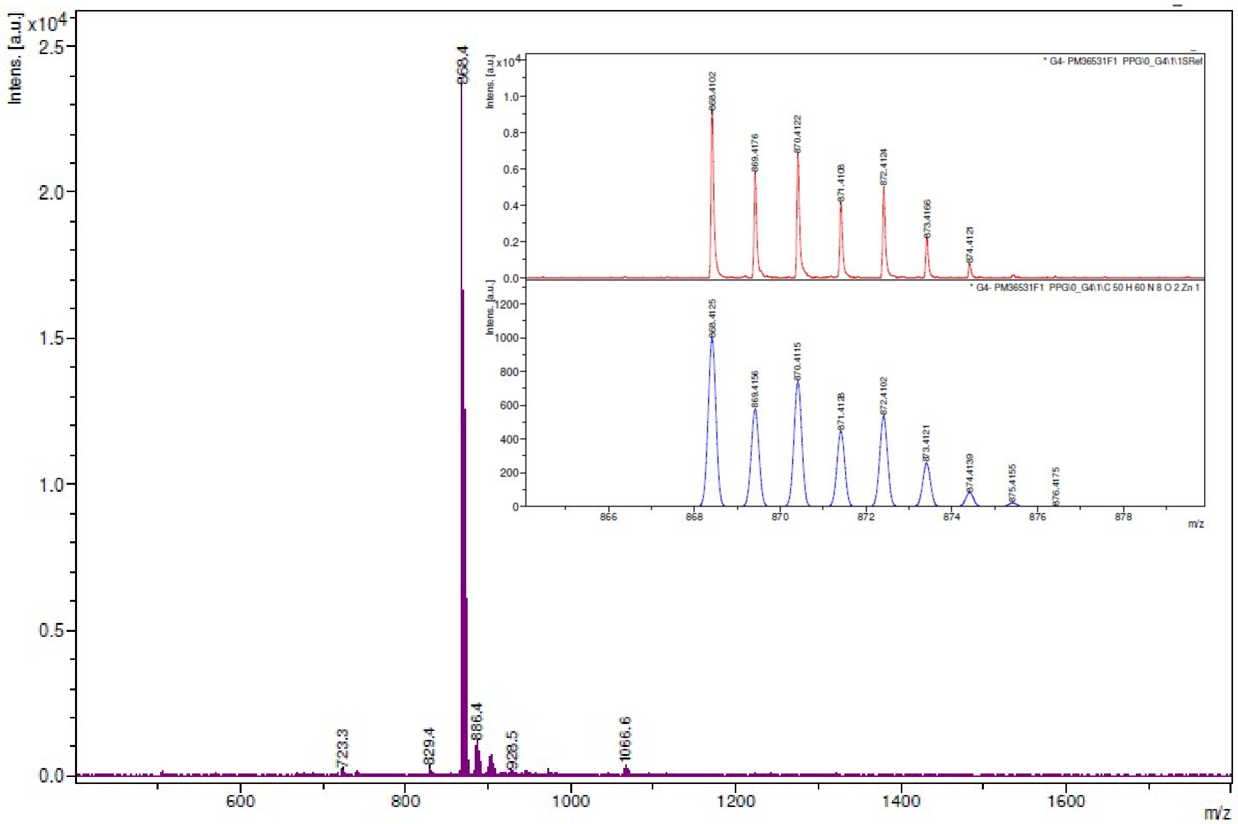

Figure S16. ^{13}C NMR spectra of **Pz2** in *d*$_8$-THF.

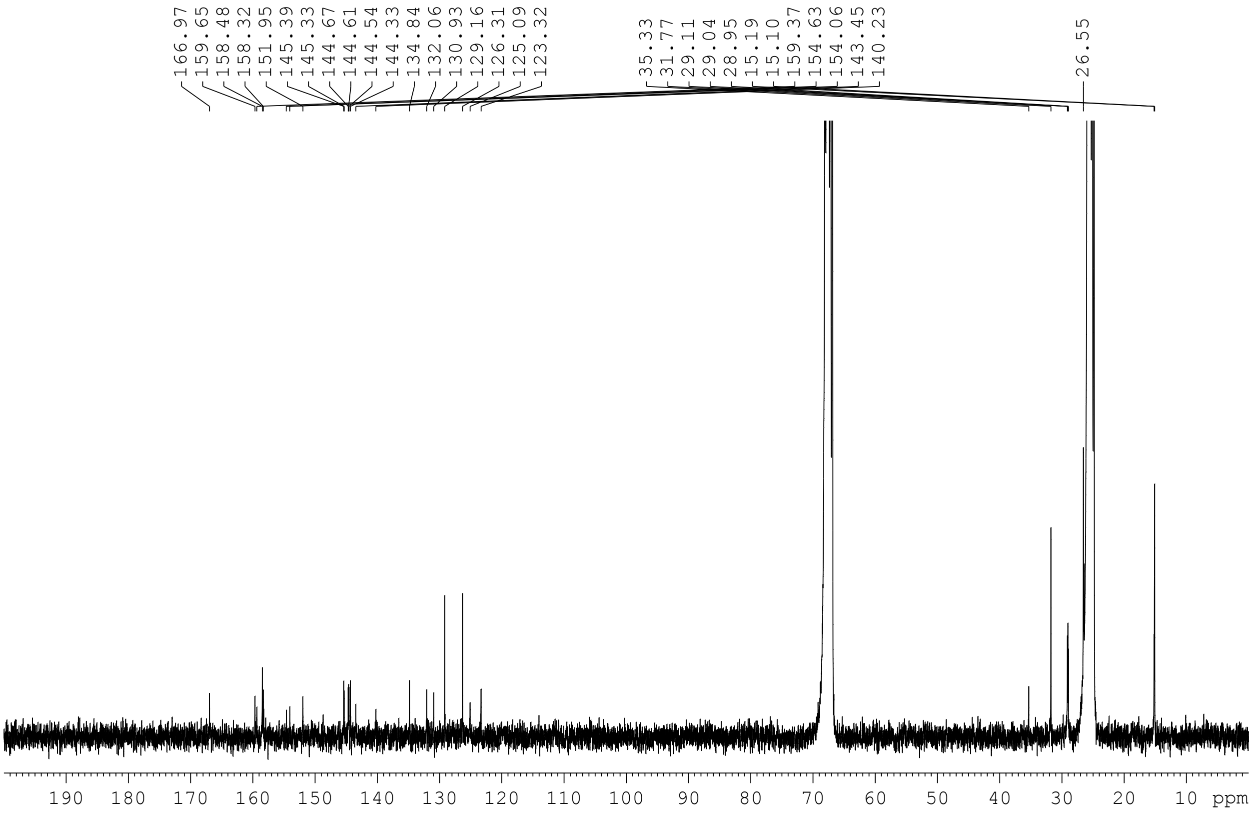

Figure S17. MS (MALDI-TOF) and HRMS spectra (inset) of **Pz2**.

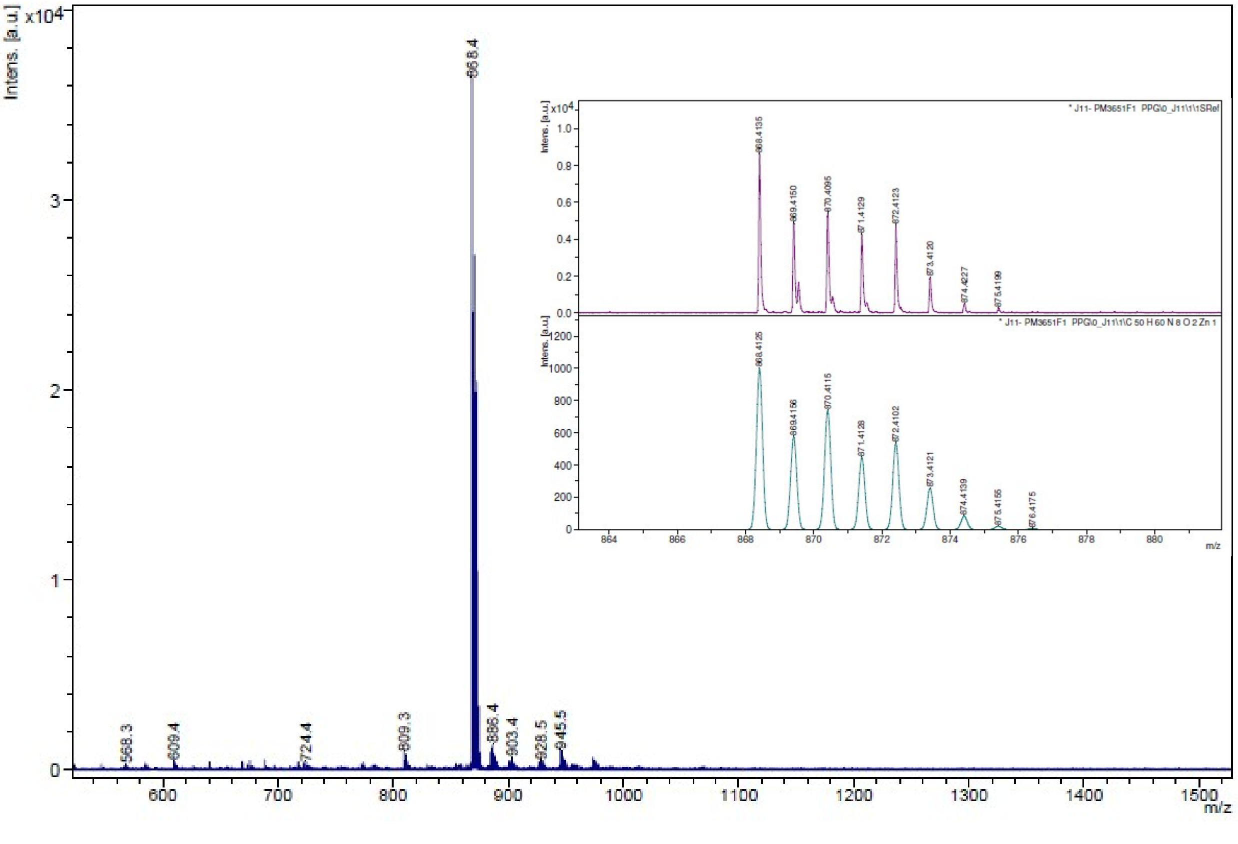

Figure S18. Steady-state absorption spectra of **Pz1** (black), **Pnc$_2$COOH** (red), and **1** (blue) in toluene (Tol).

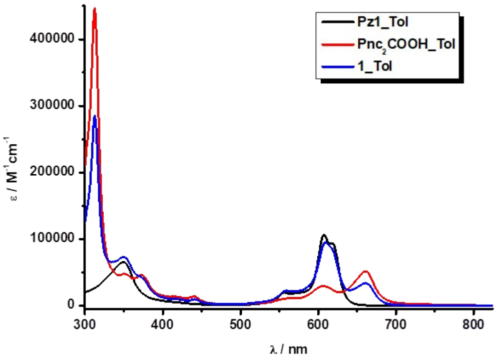

Figure S19. a) Steady-state absorption spectra of **Pz1** (black), **Pnc$_2$COOH** (red), and **1** (blue) in benzonitrile (BN). b) Normalized steady-state absorption spectra of **Pz1** (grey), **Pnc$_2$COOH** (light-grey), and **1** (black) in BN. c) Normalized steady-state fluorescence spectra of **Pz1** (grey), **Pnc$_2$COOH** (light-grey), and **1** (black) in BN. **Pnc$_2$COOH** centered absorption (~665.5 nm) and **Pz1** centered fluorescence (~626.5 nm) were used as points of normalization, respectively.

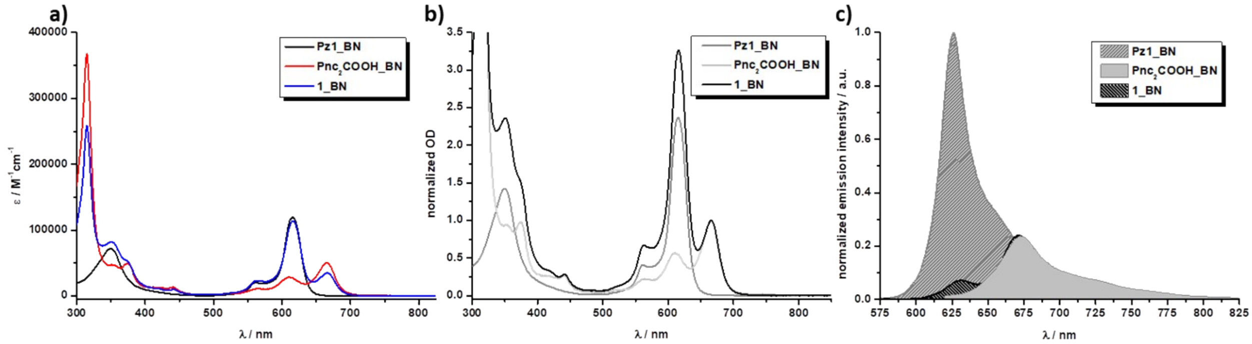

Figure S20. a) Steady-state absorption spectra of **Pz2** (black), **Pnc$_2$OH** (red), and **2** (blue) in toluene (Tol). b) Normalized steady-state absorption spectra of **Pz2** (navy), **Pnc$_2$OH** (cyan), and **2** (blue) in Tol. c) Normalized steady-state fluorescence spectra of **Pz2** (navy), **Pnc$_2$OH** (cyan), and **2** (blue) in Tol. d) Steady-state absorption spectra of **Pz2** (black), **Pnc$_2$OH** (red), and **2** (blue) in benzonitrile (BN). e) Normalized steady-state absorption spectra of **Pz2** (navy), **Pnc$_2$OH** (cyan), and **2** (blue) in BN. f) Normalized steady-state fluorescence spectra of **Pz2** (navy), **Pnc$_2$OH** (cyan), and **2** (blue) in BN. **Pnc$_2$OH** centered absorption (~659 nm in Tol, ~665 nm in BN) and **Pz2** centered fluorescence (~624 nm in Tol, ~626.5 nm in BN) were used as points of normalization, respectively.

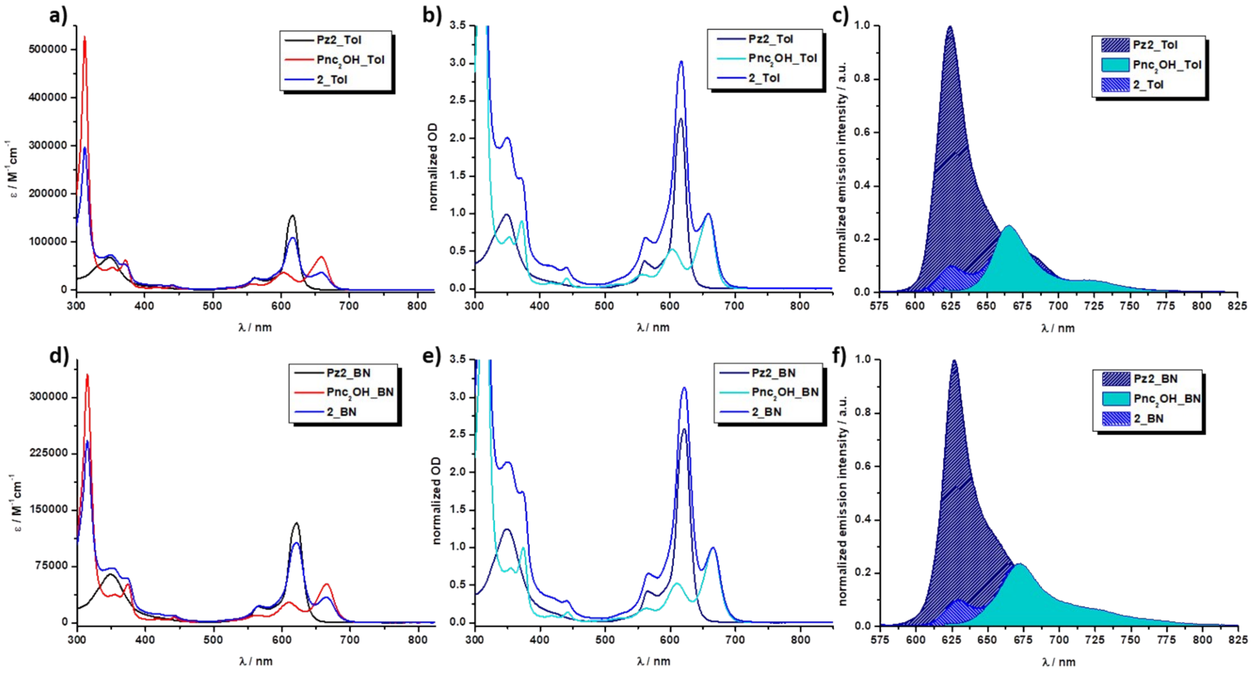

Table S1. Summary of photophysical properties of the investigated compounds in benzonitrile.

Compound	λ_{abs} / nm		λ_{em} / nm		Φ_F	τ_F
	ZnPz	**Pnc_2**	**ZnPz**	**Pnc_2**	**ZnPz[a]**	**Pz[a]**
Pnc_2COOH	-	665.5	-	672.5	~0.02[b]	<200 ps[b,c]
Pnc_2OH	-	665	-	673	~0.01[b]	<100 ps[b,c]
Pz-1	615.5	-	626.5	-	0.20	2.51 ns
Pz-2	621	-	626.5	-	0.25	2.88 ns
1	616	666	625.5	673.5	<0.01	<200 ps[c]
2	621.5	665.5	629	672.5	<0.01	<200 ps[c]

[a] Values refer to the ZnPz centered fluorescence if not stated otherwise. [b] Value refers to the pentacene (Pnc_2) centered fluorescence. [c] Lifetime is below the resolution limit of our time-correlated single photon counting (TCSPC) setup.

Figure S21. (a) – Differential absorption spectra obtained upon fsTA experiments (570 nm) of **Pz2** in toluene with several time delays between 0 and 5250 ps at rt, with the inset showing kinetics at the respective wavelengths (b) – Evolution associated spectra of the transient absorption data of **Pz2** shown in a), with the initially formed singlet excited state $^1(S_1)_{Pz2}$ (black) and triplet excited state $^3(T_1)_{Pz2}$ (orange). The inset depicts the relative populations of the respective states. (c) – Differential absorption spectra obtained upon nsTA experiments (570 nm) of **Pz2** in toluene with several time delays between 0 and 400 μs at rt, with the inset showing kinetics at the respective wavelengths (d) – Evolution associated spectra of the transient absorption data of **Pz2** shown in c), with the initially formed singlet excited state $^1(S_1)_{Pz2}$ (black) and triplet excited state $^3(T_1)_{Pz2}$ (orange). The inset depicts the relative populations of the respective states.

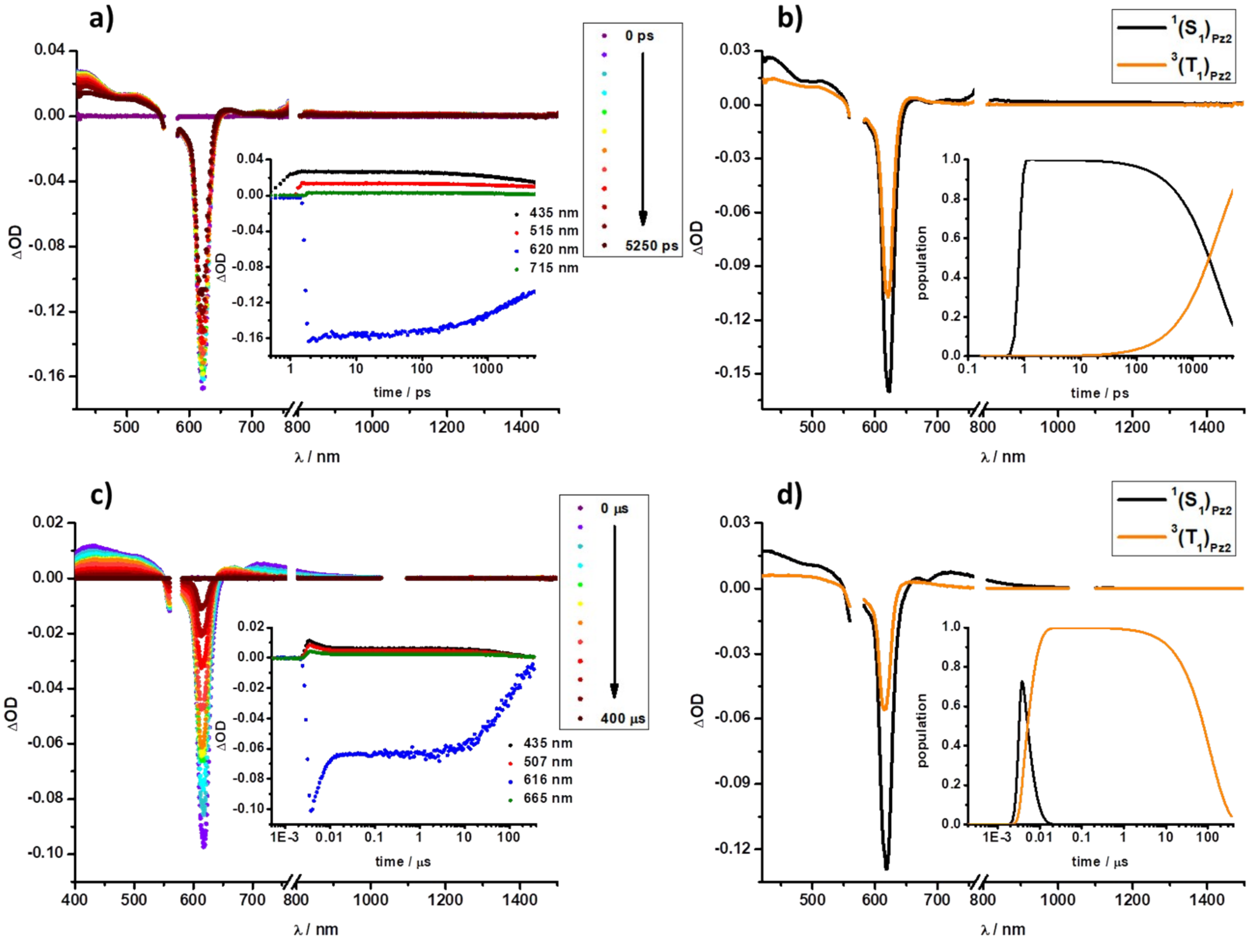

Figure S22. (a) – Differential absorption spectra obtained upon fsTA experiments (633 nm) of **Pnc$_2$OH** in toluene with several time delays between 0 and 5250 ps at rt, with the inset showing kinetics at the respective wavelengths (b) – Evolution associated spectra of the transient absorption data of **Pnc$_2$OH** shown in a), with the initially formed singlet excited state $^1(S_1S_0)_{Pnc2OH}$ (red), intermediate state $^{CT}(S_1S_0)_{Pnc2OH}$ (blue), and singlet correlated triplet pair state $^1(T_1T_1)_{Pnc2OH}$ (green). The inset depicts the relative populations of the respective states.

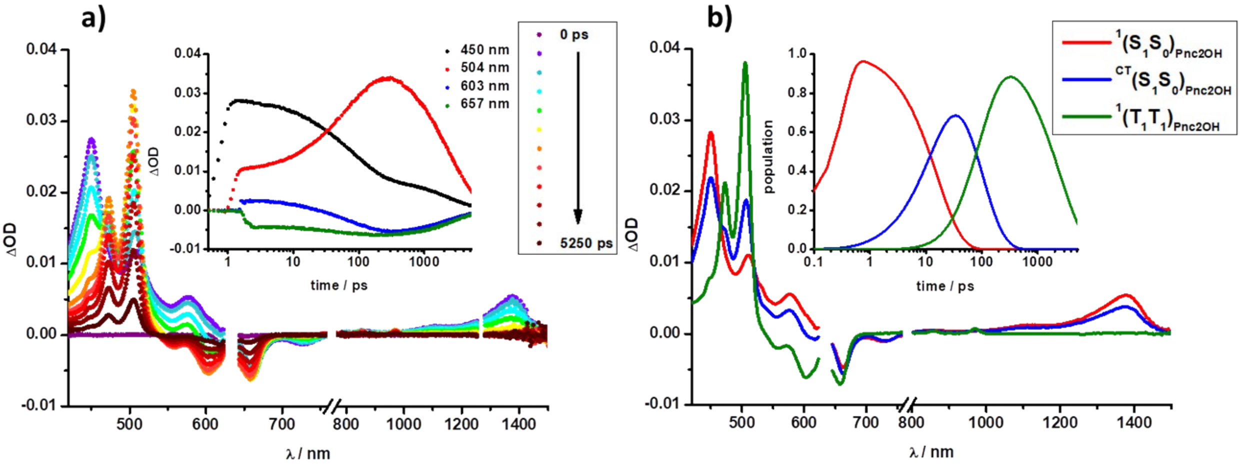

Figure S23. (a) – Differential absorption spectra obtained upon fsTA experiments (570 nm) of **2** in toluene with several time delays between 0 and 5250 ps at rt, with the inset showing kinetics at the respective wavelengths (b) – Evolution associated spectra of the transient absorption data of **2** shown in a), with the initially formed ZnPz singlet excited state $^1(S_1)_{Pz2}$ (black), the Pnc2 singlet excited state $^1(S_1S_0)_{Pnc2,2}$ (red), intermediate state $^{CT}(S_1S_0)_{Pnc2,2}$ (blue), and singlet correlated triplet pair state $^1(T_1T_1)_{Pnc2,2}$ (green). The inset depicts the relative populations of the respective states.

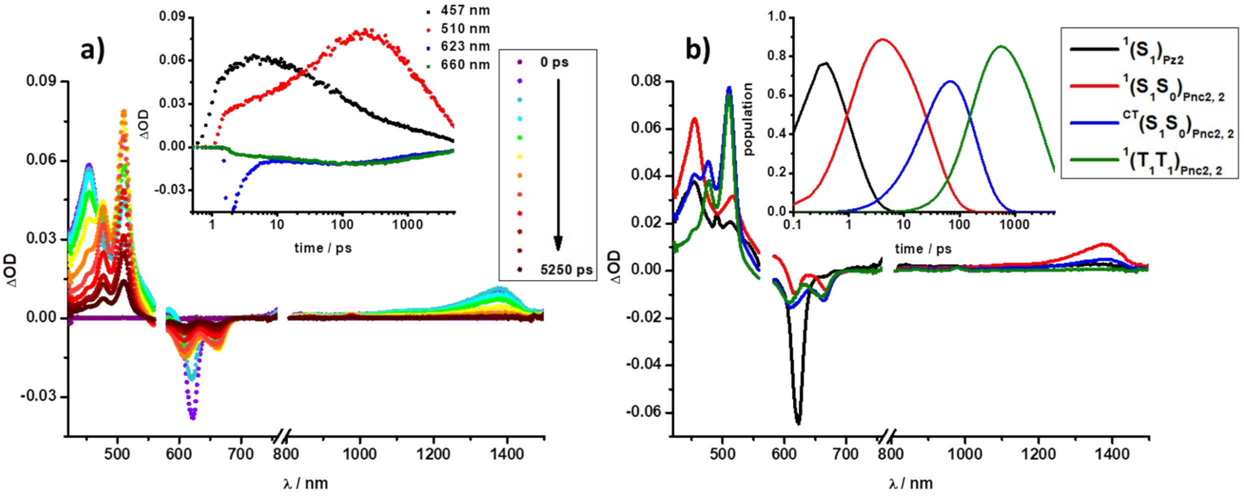

Figure S24. (a) – Differential absorption spectra obtained upon fsTA experiments (570 nm) of **Pz1** in benzonitrile with several time delays between 0 and 5250 ps at rt, with the inset showing kinetics at the respective wavelengths (b) – Evolution associated spectra of the transient absorption data of **Pz1** shown in a), with the initially formed singlet excited state $^1(S_1)_{Pz1}$ (black) and triplet excited state $^3(T_1)_{Pz1}$ (orange). The inset depicts the relative populations of the respective states. (c) – Differential absorption spectra obtained upon nsTA experiments (570 nm) of **Pz1** in benzonitrile with several time delays between 0 and 400 μs at rt, with the inset showing kinetics at the respective wavelengths (d) – Evolution associated spectra of the transient absorption data of **Pz1** shown in c), with the initially formed singlet excited state $^1(S_1)_{Pz1}$ (black) and triplet excited state $^3(T_1)_{Pz1}$ (orange). The inset depicts the relative populations of the respective states.

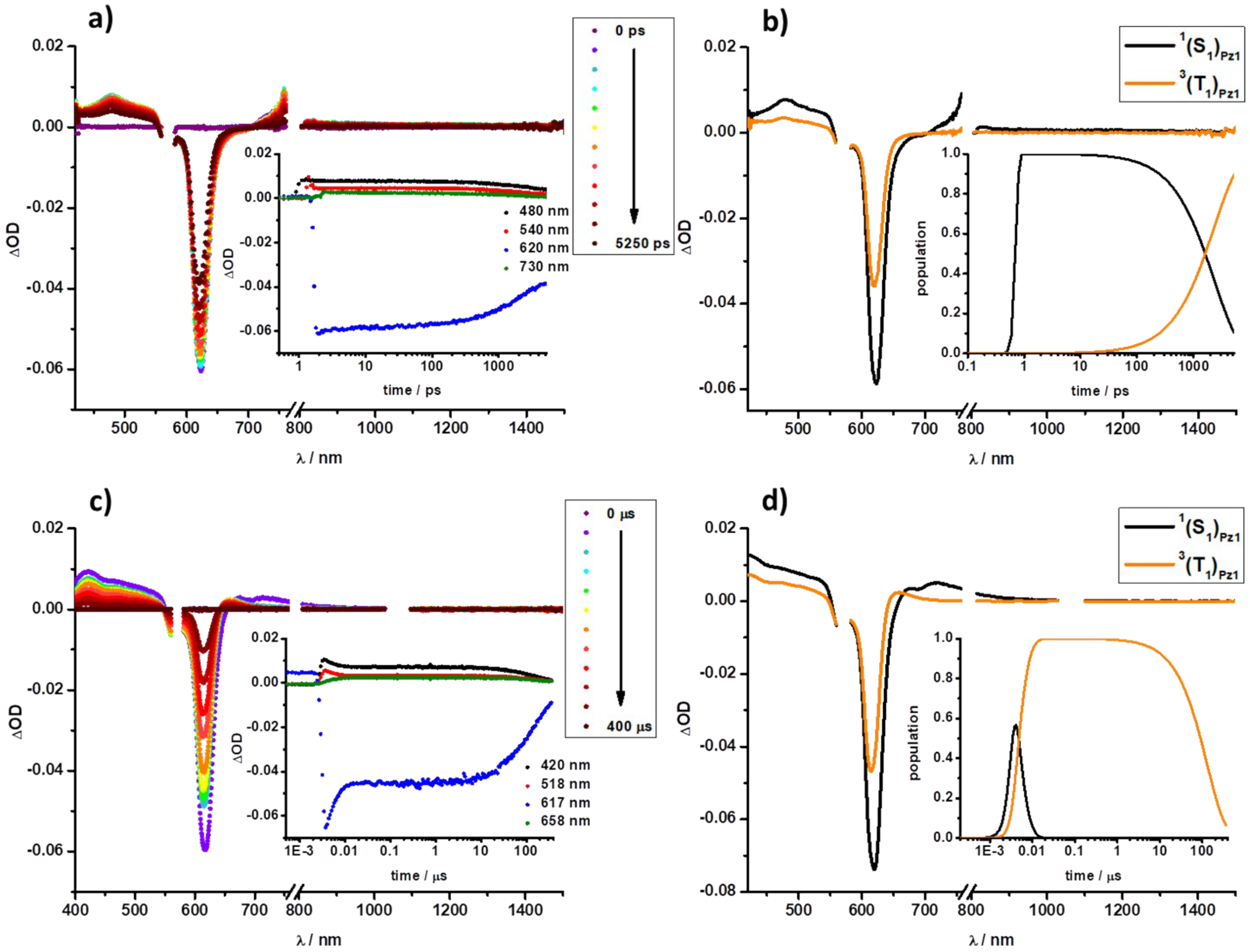

Figure S25. (a) – Differential absorption spectra obtained upon fsTA experiments (570 nm) of **Pz2** in benzonitrile with several time delays between 0 and 5250 ps at rt, with the inset showing kinetics at the respective wavelengths (b) – Evolution associated spectra of the transient absorption data of **Pz2** shown in a), with the initially formed singlet excited state $^1(S_1)_{Pz2}$ (black) and triplet excited state $^3(T_1)_{Pz2}$ (orange). The inset depicts the relative populations of the respective states. (c) – Differential absorption spectra obtained upon nsTA experiments (570 nm) of **Pz2** in benzonitrile with several time delays between 0 and 400 μs at rt, with the inset showing kinetics at the respective wavelengths (d) – Evolution associated spectra of the transient absorption data of **Pz2** shown in c), with the initially formed singlet excited state $^1(S_1)_{Pz2}$ (black) and triplet excited state $^3(T_1)_{Pz2}$ (orange). The inset depicts the relative populations of the respective states.

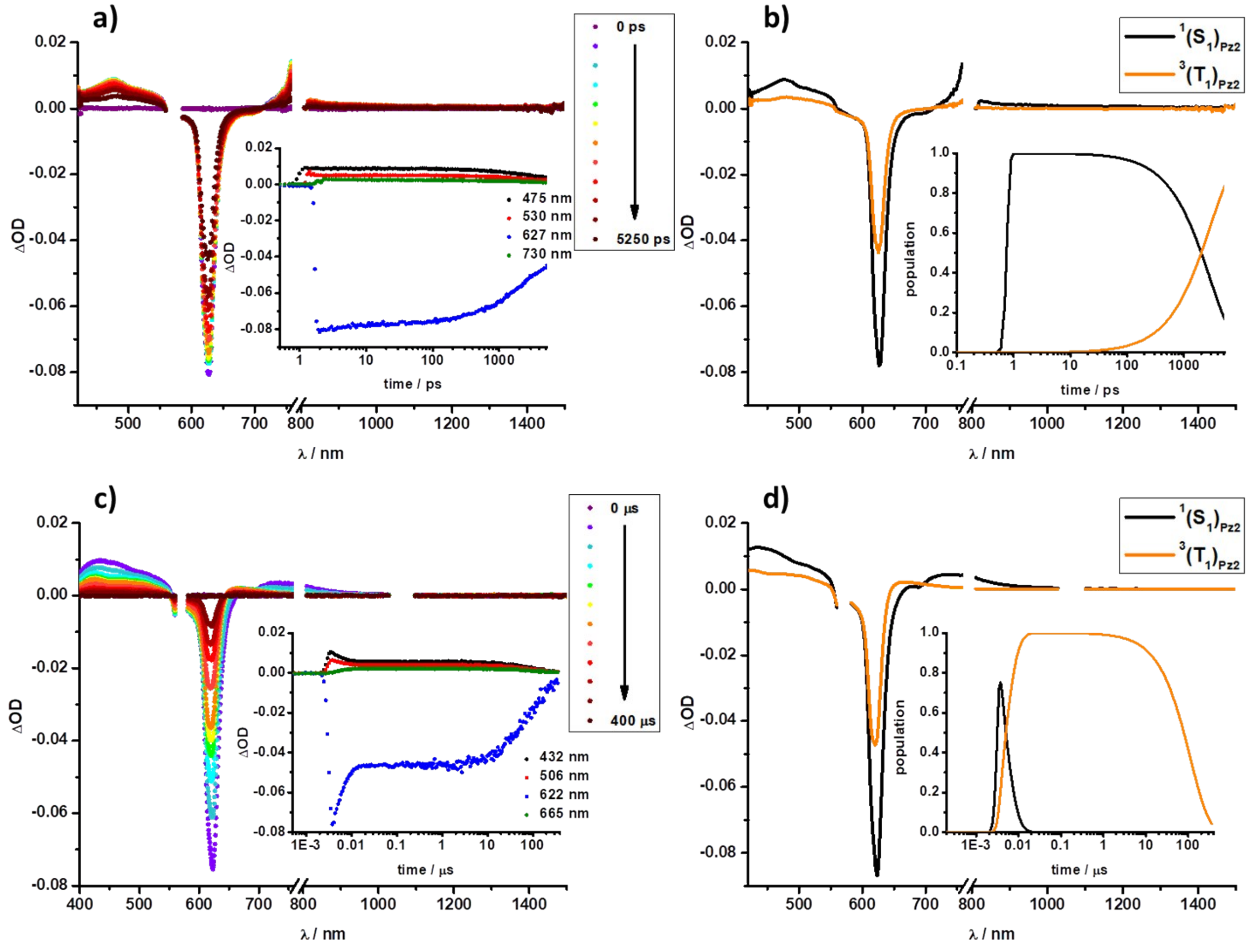

Figure S26. (a) – Differential absorption spectra obtained upon fsTA experiments (633 nm) of **Pnc$_2$COOH** in benzonitrile with several time delays between 0 and 5250 ps at rt, with the inset showing kinetics at the respective wavelengths (b) – Evolution associated spectra of the transient absorption data of **Pnc$_2$COOH** shown in a), with the initially formed singlet excited state $^1(S_1S_0)_{Pnc2OH}$ (red), intermediate state $^{CT}(S_1S_0)_{Pnc2OH}$ (blue), and singlet correlated triplet pair state $^1(T_1T_1)_{Pnc2OH}$ (green). The inset depicts the relative populations of the respective states.

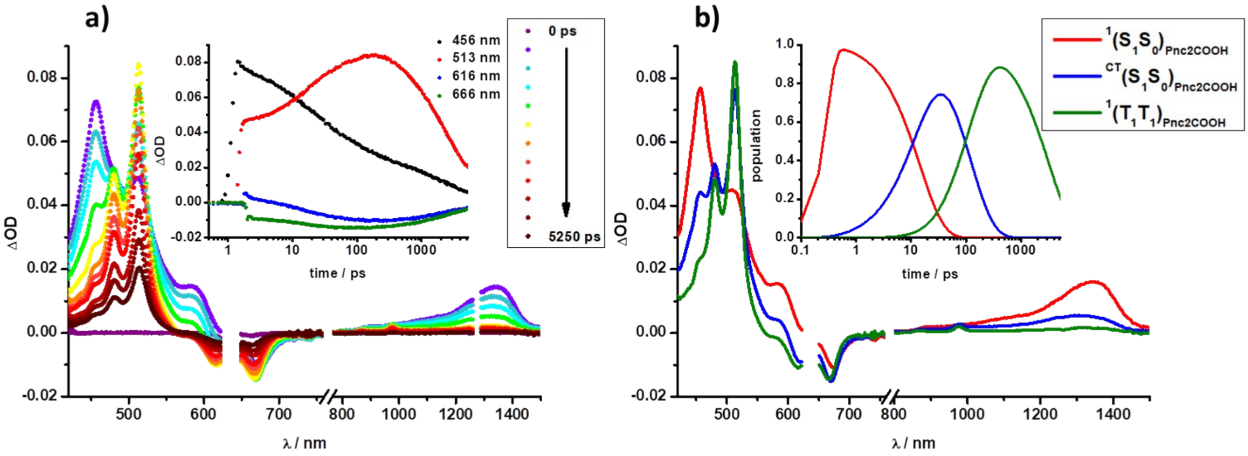

Figure S27. (a) – Differential absorption spectra obtained upon fsTA experiments (633 nm) of **Pnc$_2$OH** in benzonitrile with several time delays between 0 and 5250 ps at rt, with the inset showing kinetics at the respective wavelengths (b) – Evolution associated spectra of the transient absorption data of **Pnc$_2$OH** shown in a), with the initially formed singlet excited state $^1(S_1S_0)_{Pnc2OH}$ (red), intermediate state $^{CT}(S_1S_0)_{Pnc2OH}$ (blue), and singlet correlated triplet pair state $^1(T_1T_1)_{Pnc2OH}$ (green). The inset depicts the relative populations of the respective states.

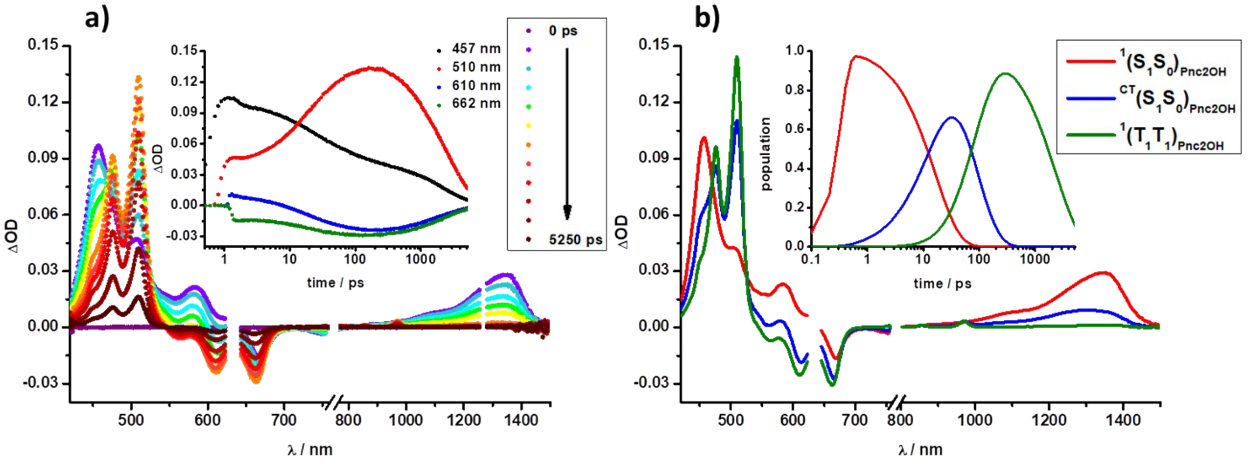

Figure S28. (a) – Differential absorption spectra obtained upon fsTA experiments (570 nm) of **1** in benzonitrile with several time delays between 0 and 5250 ps at rt, with the inset showing kinetics at the respective wavelengths (b) – Evolution associated spectra of the transient absorption data of **1** shown in a), with the initially formed ZnPz singlet excited state $^1(S_1)_{Pz1}$ (black), the Pnc2 singlet excited state $^1(S_1S_0)_{Pnc2,1}$ (red), intermediate state $^{CT}(S_1S_0)_{Pnc2,1}$ (blue), and singlet correlated triplet pair state $^1(T_1T_1)_{Pnc2,1}$ (green). The inset depicts the relative populations of the respective states.

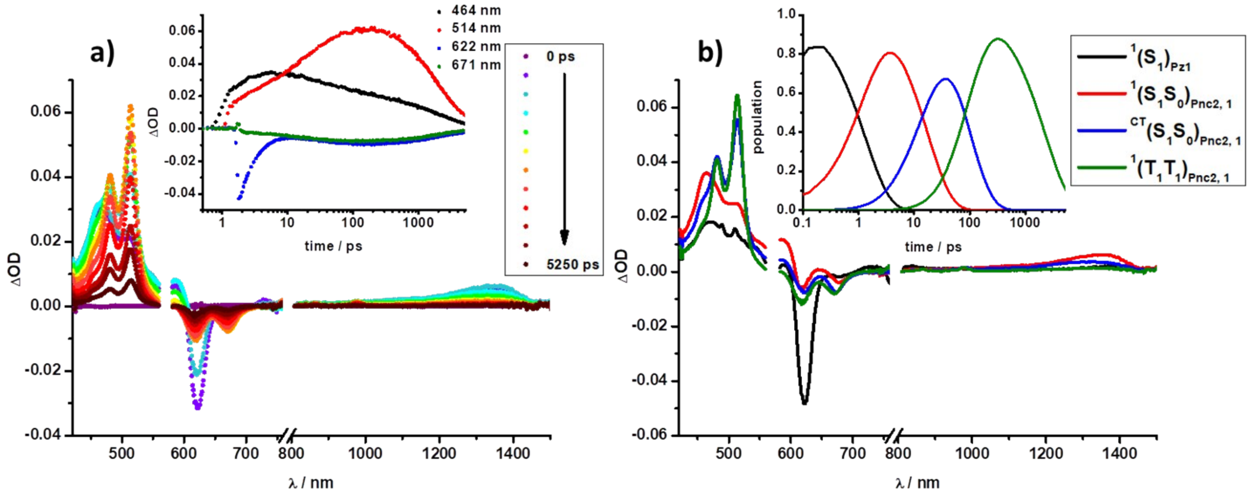

Figure S29. (a) – Differential absorption spectra obtained upon fsTA experiments (570 nm) of **2** in benzonitrile with several time delays between 0 and 5250 ps at rt, with the inset showing kinetics at the respective wavelengths (b) – Evolution associated spectra of the transient absorption data of **2** shown in a), with the initially formed ZnPz singlet excited state $^1(S_1)_{Pz2}$ (black), the Pnc2 singlet excited state $^1(S_1S_0)_{Pnc2,2}$ (red), intermediate state $^{CT}(S_1S_0)_{Pnc2,2}$ (blue), and singlet correlated triplet pair state $^1(T_1T_1)_{Pnc2,2}$ (green). The inset depicts the relative populations of the respective states.

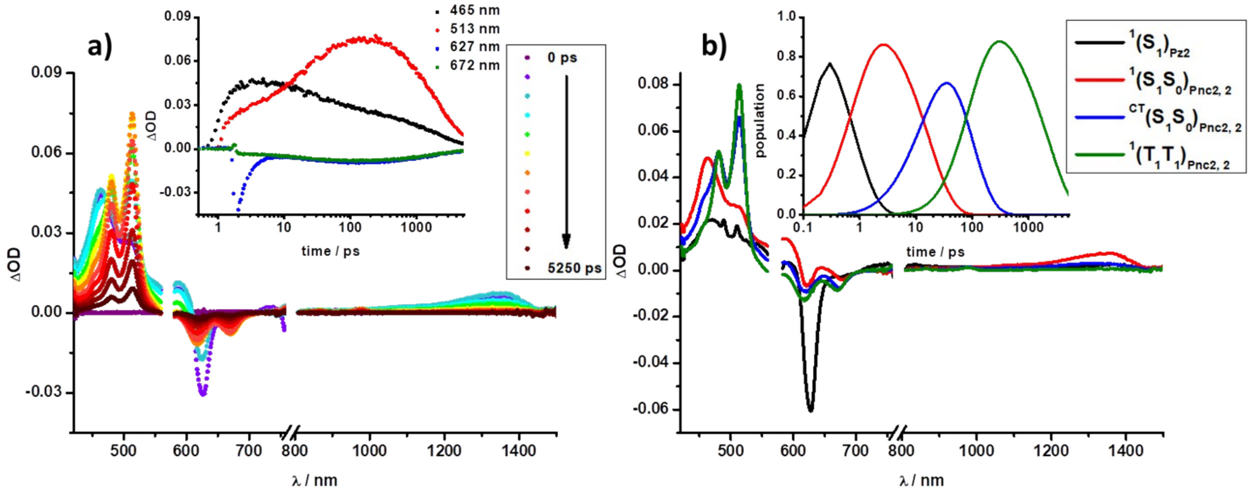

Figure S30. (a) – Evolution associated spectra of the differential absorption spectra obtained upon fsTA experiments (570 nm) of **Pnc$_2$COOH** in toluene with several time delays between 0 and 5250 ps at rt, with the initially formed ZnPz singlet excited state $^{1}(S_1S_0)_{Pnc2COOH}$ (red), intermediate state $^{CT}(S_1S_0)_{Pnc2COOH}$ (blue), and singlet correlated triplet pair state $^{1}(T_1T_1)_{Pnc2COOH}$ (green). The inset depicts the relative populations of the respective states. (b) – Respective species associated spectra and relative populations.

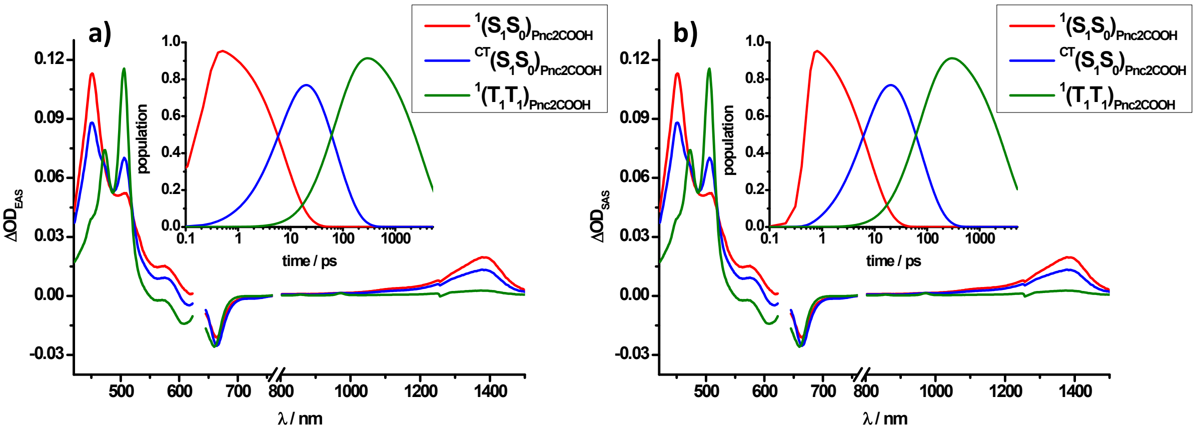

Figure S31. (a) – Evolution associated spectra of the differential absorption spectra obtained upon fsTA experiments (570 nm) of **1** in toluene with several time delays between 0 and 5250 ps at rt, with the initially formed ZnPz singlet excited state $^{1}(S_1)_{Pz1}$ (black), the Pnc$_2$ singlet excited state $^{1}(S_1S_0)_{Pnc2,1}$ (red), intermediate state $^{CT}(S_1S_0)_{Pnc2,1}$ (blue), and singlet correlated triplet pair state $^{1}(T_1T_1)_{Pnc2,1}$ (green). The inset depicts the relative populations of the respective states. (b) – Respective species associated spectra and relative populations.

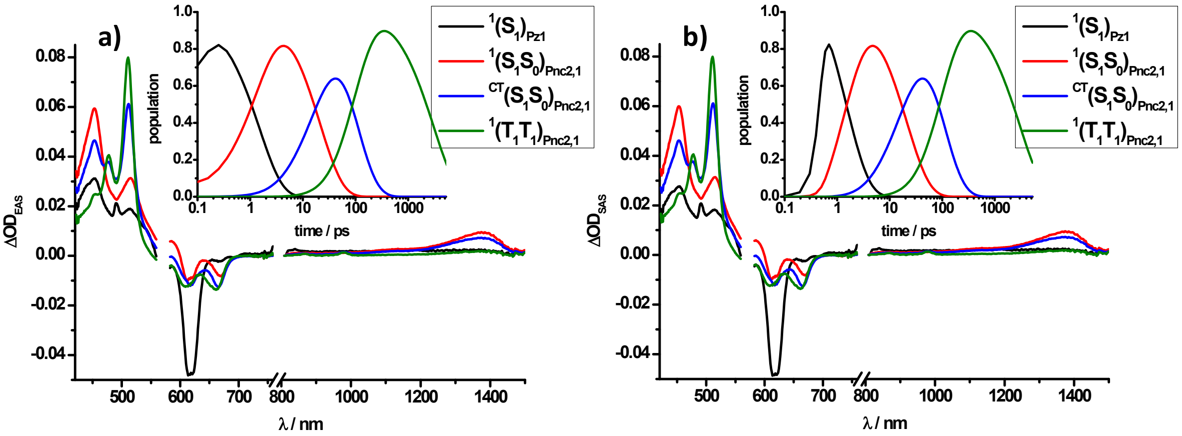

Table S2. Summary of kinetic data and triplet quantum yields (TQYs) of **Pz1**, **Pz2**, **Pnc$_2$COOH**, **Pnc$_2$OH**, **1**, and **2** obtained from fsTA and nsTA in benzonitrile.

	fsTA					nsTA	
Compound	$^1(S_1)_{Pz}$	$^1(S_1S_0)_{Pnc2}$	$^{CT}(S_1S_0)_{Pnc2}$	$^1(T_1T_1)_{Pnc2}$	TQY[a,b]	$^1(S_1)_{Pz}$	$^3(T_1)_{Pz}$
Pz-1	2.32 ns	-	-	-	-	2.42 ns	129.98 µs
Pz-2	2.90 ns	-	-	-	-	2.97 ns	145.64 µs
Pnc$_2$COOH	-	14.52 ps	116.03 ps	3.24 ns	132% ±20%	-	-
Pnc$_2$OH	-	16.30 ps	78.28 ps	2.31 ns	186% ±20%	-	-
1	1.34 ps	17.25 ps	88.70 ps	2.31 ns	206% ±20%	n.r.[c]	-
2	0.77 ps	16.94 ps	83.92 ps	2.21 ns	176% ±20%	n.r.	-

[a] Determined via following the intensification of the transient bleaching of the Pnc$_2$ moiety and comparing the relative intensification of the evolution-associated for the $^1(S_1S_0)_{Pnc2}$ and the $^1(T_1T_1)_{Pnc2}$ state, respectively. [b] An error margin in the range of ±20% may be considered when determining the TQYs. [c] n.r. = not resolvable. Lifetimes are either too long to be resolved with fsTA or too short to be resolved with nsTA.

---

[1] J. Fernández-Ariza, M. Urbani, M. Grätzel, M. S. Rodríguez-Morgade, M. K. Nazeeruddin, T. Torres, *ChemPhotoChem*, 2017, **1**, 164-166.

[2] A. Kunzmann, M. Gruber, R. Casillas, J. Zirzlmeier, M. Stanzel, W. Peukert, R. R. Tykwinski and D. M. Guldi, *Angew. Chem. Int. Ed.*, 2018, **57***,* 10742.

[3] H. Gotfredsen, PhD Thesis, University of Copenhagen, Denmark, 2018.

[4] S. J. Lange, H. Nie, C. L. Stern, A. G. M. Barrett, B. M. Hoffman, *Inorg. Chem.*, 1998, **37**, 6435-6443.

[5] G. Pozzi, S. Quici, M. C. Raffo, C. A. Bignozzi, St. Caramori, M. Orlandi, *J. Phys. Chem. C*, 2011, **115**, 3777-3788.